Litter quality outweighs climate as a driver of decomposition across the tundra biome

Thomas, Haydn J. D.[1]; Myers-Smith, Isla H.[1,2]; Borderieux, Jeremy[2] ;Høye, Toke T.[3]; Petit Bon, Matteo[4,5].; Lembrechts, Jonas[6]; Walker, Eleanor R.[1]; Björnsdóttir, Katrín[7,8]; Barrio, Isabel C.[9]; Jónsdóttir, Inga Svala[7]; Venn, Susanna[10]; Alatalo, Juha M.[11]; Baltzer, Jennifer L.[12], Wallace, Cory A.[12]; Ackerman, Daniel E.[13]; Gough, Laura[14]; Prevéy, Janet S.[15,16]; Rixen, Christian[16]; Carbognani, Michele[17]; Petraglia, Alessandro[17]; Christiansen, Casper T.[18]; Inouye, David W.[19,20]; Ogilvie, Jane E.[20]; Trouillier, Mario[21]; Wilmking, Martin[21]; Treharne, Rachel[22]; Angers-Blondin, Sandra[1]; Urbanowicz, Christine[23]; von Oppen, Jonathan[3,16]; Wipf, Sonja[16]; Smith, Paul A.[24]; Suzuki, Satoshi N.[25]; Suzuki, Ryo O.[26].; Virkkala, Anna-Maria[27]; Luoto, Miska[27]; Serikova, Svetlana[28]; Bjorkman, Anne D.[8,29]; Blok, Daan[30]; Gallois, Elise C.[1]; Sarneel, Judith M.[28]

1. School of Geosciences, University of Edinburgh, UK
2. Department of Forest and Conservation Sciences, Faculty of Forestry, University of British Columbia, Vancouver, Canada
3. Aarhus University, Denmark
4. University Centre in Svalbard, Svalbard
5. Arctic University of Norway, Norway
6. University of Antwerp, Belgium
7. University of Iceland, Iceland
8. University of Gothenburg, Sweden
9. Agricultural University of Iceland, Iceland
10. Deakin University, Australia
11. Qatar University, Qatar
12. Wilfrid Laurier University, Canada
13. University of Minnesota, USA
14. Towson University, USA
15. USDA Forest Service Pacific Northwest Research Station, Washington, USA
16. WSL Institute for Snow and Avalanche Research SLF, Switzerland
17. University of Parma, Italy
18. Bjerknes Centre for Climate Research, Norway, Norway
19. University of Maryland, USA
20. Rocky Mountain Biological Laboratory, Colorado, USA
21. University of Greifswald, Germany
22. University of Sheffield, UK

38 23. Dartmouth College, New Hampshire, USA
39 24. Environment and Climate Change Canada, Canada
40 25. University of Tokyo, Japan
41 26. University of the Ryukyus, Japan
42 27. University of Helsinki, Finland
43 28. Umeå University, Sweden
44 29. Senckenberg Gesellschaft für Naturforschung, Biodiversity and Climate Research Centre (BiK-F),
45 Germany
46 30. Lund University, Sweden

47

48 Author contributions: HT and IMS conceived the study, IMS supervised the research. JS
49 devised and helped to adapt the Tea Bag Index for tundra settings. Data were collected by all
50 authors except AB, DB, JB and JS. HT compiled the tundra teabag dataset. HT and AB
51 performed statistical analysis. HT wrote the manuscript with input from IMS, JB, AB, EG, JvO,
52 KB and contributions from all authors.

53

79 **Abstract**

80 Considerable uncertainty exists regarding the strength, direction and relative importance of
81 the drivers of decomposition in the tundra biome, partly due to a lack of coordinated
82 decomposition field studies in this remote environment. Here, we analysed 3717 incubations
83 of two uniform litter types, green and rooibos tea, buried at 330 circum-Arctic and alpine sites
84 to quantify the effects of temperature, moisture and litter quality on decomposition. We found
85 a surprisingly linear positive relationship between decomposition and soil temperature across
86 all sites, counter to theory and previous model estimates. Litter mass loss was greater at
87 wetter sites, even where soils reached almost full water saturation. However, litter quality was
88 the strongest driver of litter mass loss across the tundra biome, explaining six times more
89 variation in summer decomposition than soil temperature. Our results indicate that climate
90 warming will directly increase decomposition across tundra environments. Yet, the indirect
91 effects of climate change on vegetation communities, and thus plant litter inputs and quality,
92 could have a more profound impact than direct effects on the balance of this globally important
93 carbon store.

94

95 **Introduction**

96 The decomposition of terrestrial carbon pools is a vital component of the global carbon cycle[1,2]
97 and is sensitive to temperature[3]. Climate warming is predicted to accelerate both the
98 decomposition process and carbon emissions[2,4,5]. Quantifying changes in decomposition is
99 thus critical for identifying major feedbacks to climate change[6]. Perhaps nowhere is this more
100 true than in high-latitude ecosystems, which contain over a third of global soil carbon[7–9], more
101 than double the current atmospheric stocks[10]. Decomposition in the tundra is currently
102 constrained by cold temperatures, frozen soils and recalcitrant litter, encouraging the build-up
103 of organic matter in soils[11]. Tundra ecosystems are warming at up to four times the global
104 average rate[12], with annual temperatures in the Arctic predicted to increase by 2-10°C by the
105 end of the century relative to the period from 1850 to 1900[13]. As a result, decomposition rates
106 are expected to increase in the tundra [11], potentially releasing 37 to 174 Pg of carbon by 2100,
107 equivalent to an additional 17 to 82 ppm CO_2 in the Earth's atmosphere[14]. Climate warming
108 impacts can either directly reduce carbon stores by accelerating decomposition[11], or indirectly
109 by changing plant litter inputs[15,16]. In addition, warming impacts on decomposition are not
110 occurring in isolation from other environmental change including changes to soil moisture[17,18].
111 Arctic carbon emissions could determine whether soils globally are a sink or source of carbon
112 under accelerating global change[6]. Thus, there is an urgent need to explore the drivers of
113 decomposition across the tundra biome.

114

Despite the potential substantial impact of climate change on carbon cycling in Arctic terrestrial ecosystems, the relative influence of environmental drivers of decomposition have yet to be experimentally tested at the tundra biome scale. Temperature and soil moisture are considered to be the primary drivers of decomposition[11], and together explain approximately 70% of variation in decomposition rates globally[2,19,20]. However, biogeochemical models incorporate substantially different relationships between decomposition, temperature and soil moisture, particularly at climatic extremes[21] (Fig. 1). Earth system model relationships between temperature and decomposition rate are either assumed to exponentially decline or saturate near zero at sites with colder temperatures and relationships with moisture vary between saturating, optimal, linear or sigmoidal relationships[22] (Fig. 1). This lack of consistency in the assumed relationships between both soil temperature and moisture and decomposition is partly driven by a lack of *in situ* data from high-latitude regions[5,22], and contributes to the large uncertainty surrounding predictions of global soil carbon losses[4,5]. Thus, reducing this uncertainty requires *in situ* decomposition data across a range of temperature and moisture conditions within the tundra biome.
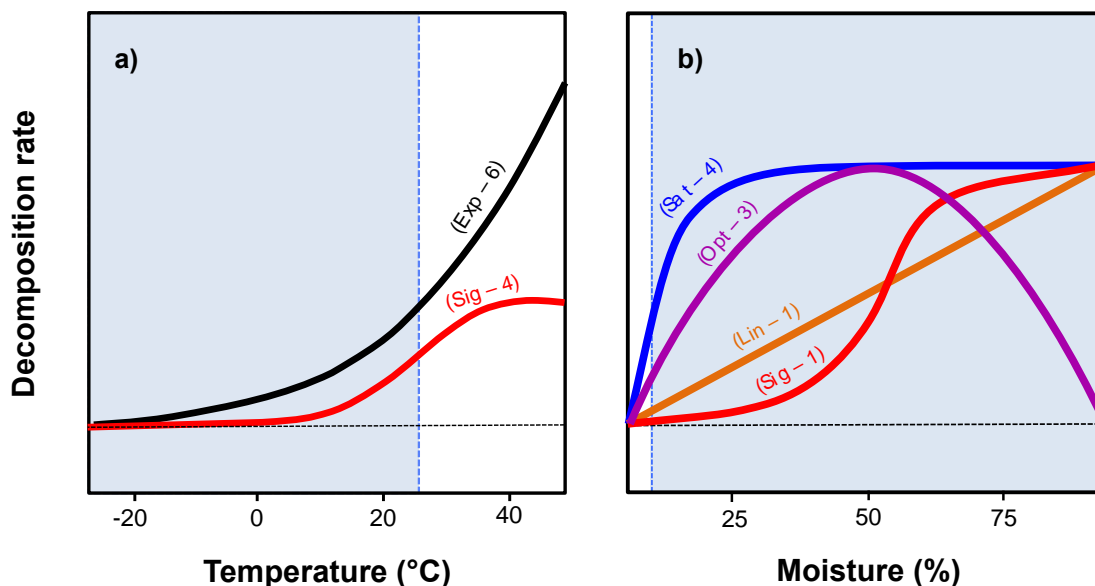
Figure 1. Biogeochemical models include a number of different shapes of relationships between decomposition rate of soil organic matter and temperature (a) and moisture (b). Summary of 19 biogeochemical model functions included in Sierra et al. 2015. The relationship between decomposition and temperature is modelled as exponential (Exp: black, six models) or sigmoidal (Sig: red, four models). The relationship between decomposition and moisture is modelled as saturating (Sat: blue, four models), optimal (Opt: purple, three models), linear (Lin: orange, one model) or sigmoidal (Sig: red, one model). The blue shaded area indicates the range of temperatures and soil moisture values for the 330 sites included in this study. Note that temperature conditions generally do not exceed ~25°C in the tundra biome.

Soil organic matter has many forms, one of which is leaf litter deposited on the soil surface and incorporated into the soil profile over time including through cryoturbation processes in tundra ecosystems[23]. Decomposition of leaf litter is dependent on litter quality, and thus the structural and chemical traits of plant tissues of different species across ecological communities[24–28]. Plant traits and litter characteristics may be the dominant control on litter decomposition worldwide, outweighing environmental drivers even across biomes[25,29,30]. As plant community composition changes with warming, so too will the litter inputs to the soil and decomposition rates of soil organic matter[15]. Many tundra plant communities are undergoing widespread changes[31,32], notably an expansion of shrub species[33,34], that could dramatically alter litter inputs to soils[16]. Site-scale experiments indicate that litter quality explains more variation in litter decomposition than environmental variables[26,35,36]. Cross-site studies of decomposition using common substrates have been conducted for other global biomes[20,22,25,29,30,37–39]. However, the relative influence of litter quality versus environmental controls on decomposition has not yet been tested across the tundra biome, primarily due to difficulties of controlling for litter homogeneity.

In this study, we quantify the drivers of litter decomposition at 330 sites across the circum-Arctic and alpine tundra (Table S1) and 3717 incubations using the Tea Bag Index[19]. The Tea Bag Index is a standardised protocol that employs two commercially available types of tea (labile green and recalcitrant rooibos tea) to estimate stabilisation factor (S) and decomposition rate (k) and provide a chemically validated [40] and highly replicable method for measuring leaf litter decomposition across sites[19,29,41–43]. Decomposability of the two tea types is also representative of leaf litters for a range of tundra species (Fig. 2, Fig. S1) and thus provides an analogue for the potential impact of plant community change on litter decomposability in tundra ecosystems[15,28,40,44–46]. Due to relationships described in theoretical and experimental studies[2,21,22,26], we predict that decomposition will increase exponentially with temperature, and that temperature will be the strongest driver of decomposition across the broad biogeographical gradients of the tundra biome.
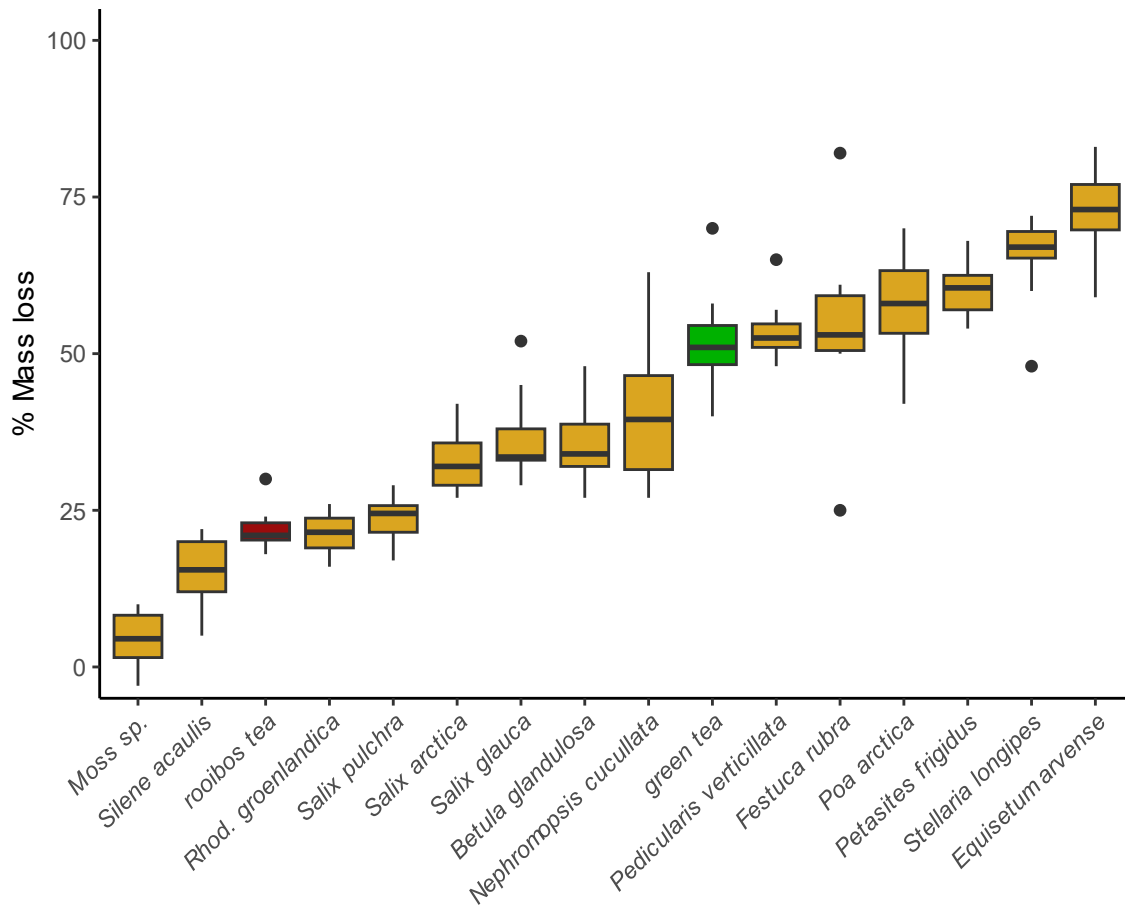
Figure 2. Annual mass loss of green and rooibos tea compared to mass loss of a range of representative tundra species. Tea types are indicated by red (rooibos tea) and green (green tea) boxplots. Tundra species were collected from two sites: the Kluane Range Mountains, Yukon, Canada (62°N) and Qikiqtaruk-Herschel Island, Yukon, Canada (70°N). All litter and tea were decomposed for one year in a common litter bed at 5-8cm depth at Kluane Lake following methods outlined in Cornelissen et al. (2007), with 10 replicates per species' litterbag and tea type. Methods are described in the Decomposition experiment section.

Results

We found that summer mass loss increased linearly with soil temperature (Fig. 3b) across tundra sites by 1.94% ± 0.31% per °C for labile green tea and 1.09% ± 0.29% per °C for recalcitrant rooibos tea, even when including a polynomial term (that allows for exponential relationships) in the models (Fig. S2). Relationships were consistent across incubation periods (Figs. S3-S4) and decomposition metrics (Figs. S5-S6), with higher temperatures associated with a lower stabilisation factor (S) and a faster decomposition rate (k). Within-site mass loss also increased with soil temperature (Fig. S7).
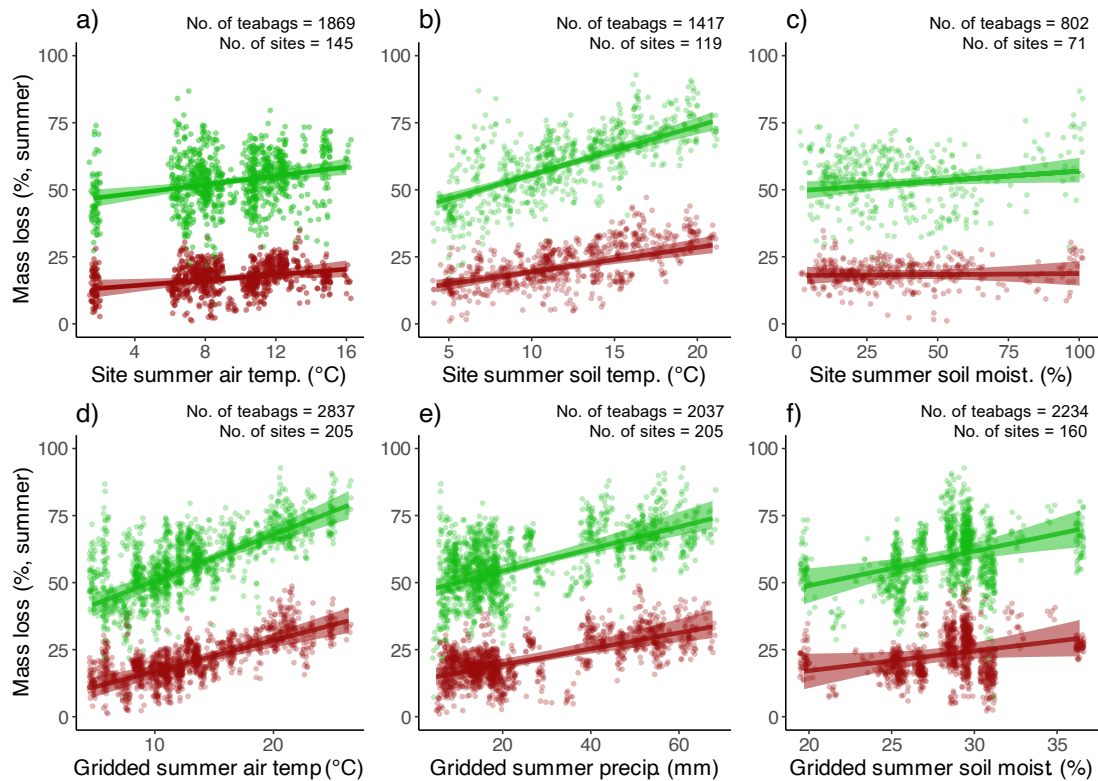
Figure 3. Relationships between litter decomposition, climate and environmental variables were linear across the range of environmental conditions found across study sites (see also Figs. S2 and S8 for non-linear models). Plotted relationships are between litter decomposition (mass loss), locally-measured environmental variables (a-c) and gridded climate data (d-f) for the summer incubation period (see also Fig. S3 for winter incubations and Fig. S4 for year-long incubations). Points indicate individual tea bag replicates across all sites. Lines indicate hierarchical Bayesian model fit with 95% credible intervals. Colours indicate tea type (red = rooibos tea, green = green tea). See Table S2 for model outputs, and Table S3 and Fig. S2 for results assuming polynomial relationships. Methods are detailed in the Environmental relationships section.

Summer mass loss increased with locally measured soil moisture across tundra sites (green tea: 0.07% ± 0.06% per % moisture, rooibos tea 0.01% ± 0.06% per % moisture, Fig. 3c).

Relationships for winter and year-long incubations were weaker than for summer incubations (Figs. S3-4). Mass loss showed a weak positive relationship with soil moisture within sites (Fig. S9). Soil moisture did not influence the relationships between soil temperature and mass loss, but litter mass loss was higher at wetter versus drier sites at any given temperature (Fig. S9).

Relationships across sites were best explained by linear, rather than polynomial relationships for temperature (Fig. S2), although relationships of green tea summer mass loss with site air temperature and soil moisture showed weak signs of saturation and an exponential

8

relationship, respectively (Fig. S2a,c). In the Eastern Hemisphere, we found an exponential relationship with soil moisture that was driven by high mass loss despite high soil moisture at sites on Svalbard, while the relationship was best explained by a linear model in the Western Hemisphere (Fig. S8).

Litter quality was the strongest predictor of litter decomposition (Fig. 4a-c), explaining six and ten times more variation in summer mass loss than soil temperature and soil moisture, respectively. This strong effect of litter quality was maintained across incubation periods (Fig. 4d-f) and mass loss of the two tea types did not converge after two years (Fig. S10).
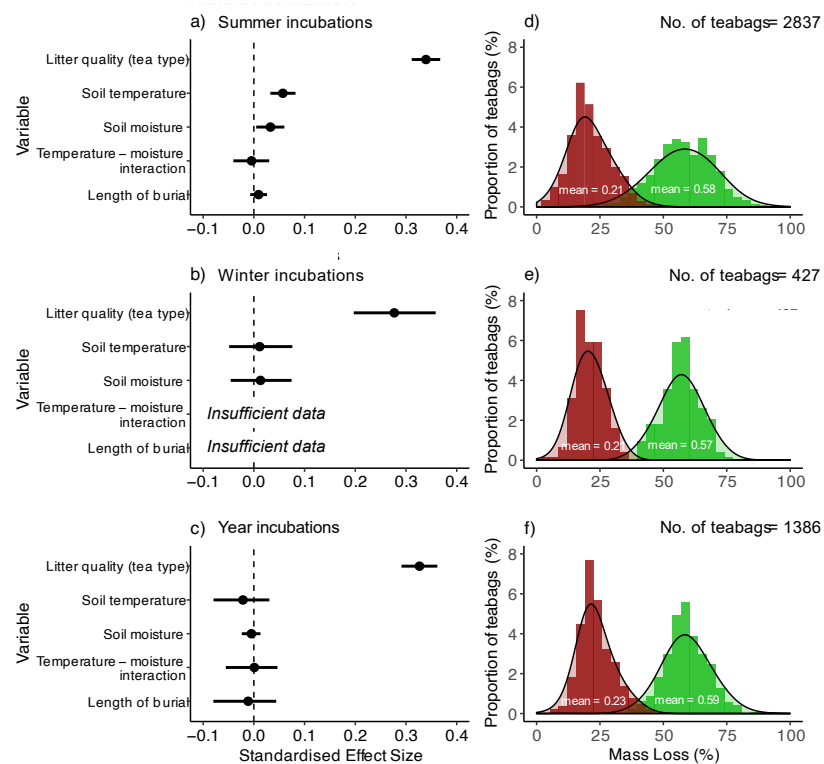
Figure 4. Litter quality explained greater variation in litter mass loss than environmental variables. Standardised effect sizes of locally measured environmental variables and litter substrate for summer incubations, winter incubations and year incubations (a-c). We did not have enough variation in incubation period to calculate the effect of length of burial (days within each incubation period) and the dataset was not large enough to test for a temperature-moisture interaction for winter incubations. Distribution of mass loss values for the two litter substrates (rooibos tea – red, green tea – green) for summer, winter and year incubations (d-f). Methods are detailed in the Environmental relationships – temperature moisture interaction section.

Relationships using gridded climate data were consistent with site-level climate data (Figs. 3, S3 and S4). We found strong linear relationships between decomposition and all gridded climate variables (Fig. 3d-f) and the interaction between gridded temperature and moisture

9

similarly suggested greater mass loss in wetter sites (Fig. S9). Extrapolating relationships across tundra and subarctic regions based on gridded climate and soil moisture revealed strong spatial variation in decomposition along biogeographic gradients (Fig. 5).
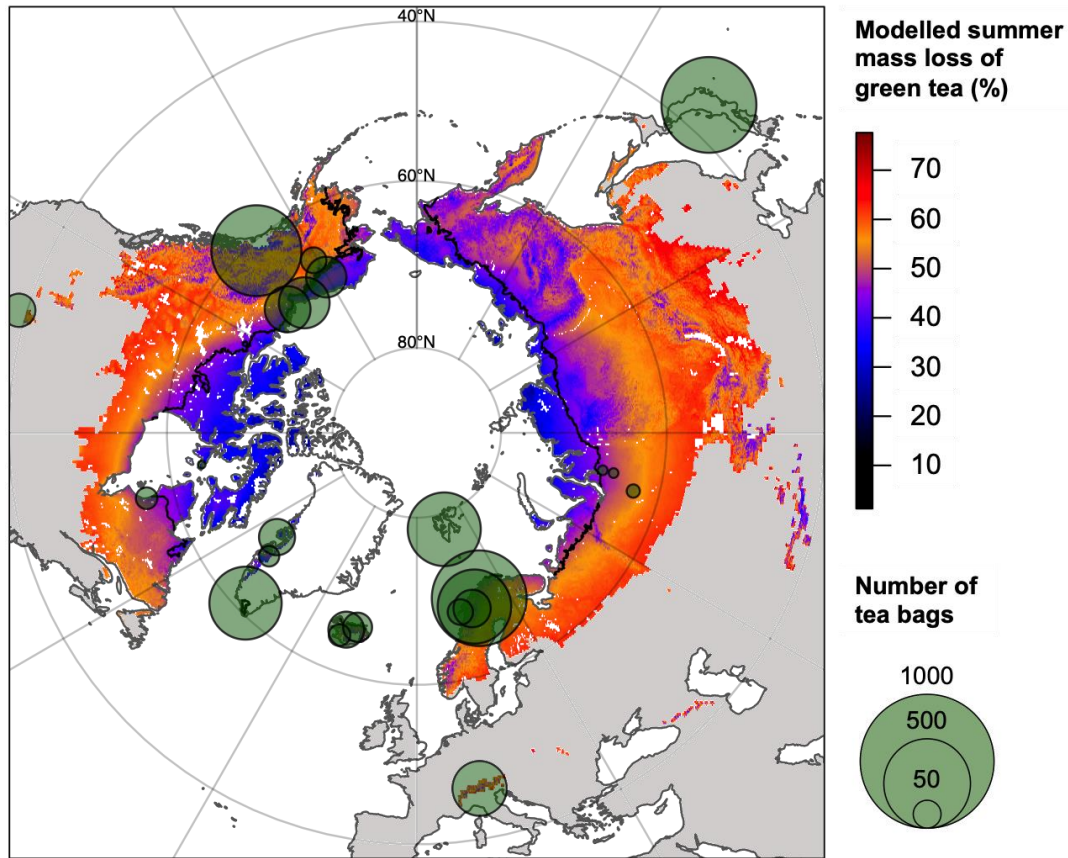
Figure 5. Modelled summer decomposition (percent mass loss) of green tea for tundra and sub-Arctic regions based on 1979 to 2013 mean summer air temperature (Climatologies at high resolution for the Earth's land surface, CHELSA) and soil moisture (European Space Agency data, ESA) from 1979 to 2013. Field collection locations are illustrated by green circles, grouped by geographic region (Table S1, figure excludes Australian alpine region). Circle size indicates the number of tea bag replicates within each geographic region. Tundra and sub-Arctic classifications are based on Köppen-Geiger classification[47]. Ice-covered areas are excluded. The circum-Arctic treeline is indicated with a black line[48]. Methods in the Mapping decomposition section.

Discussion

Contrasting with theory and model estimates, we find strong linear relationships, rather than exponential, between decomposition and summer soil temperature and moisture across the tundra biome (Fig. 3). Our findings provide comprehensive evidence that climate-driven changes to plant communities, and thus litter quality, could have a greater impact on litter decomposition than the direct effects of warming in the tundra (Fig. 4). Our results align with site-specific studies that find that decomposition is more strongly influenced by litter quality

than climatic variability[15,26–29,35,36,46,49]. Many sites across the tundra are currently undergoing rapid vegetation change[31,32,50,51], notably an increase in shrub species with relatively recalcitrant litter, which in many cases are out-competing graminoids with relatively labile litter[33,34]. This vegetation change has been hypothesised to partly counteract the effects of warming on litter decomposition[16]. Our results suggest that the biotic effects of vegetation change could outweigh the direct effects of warming on tundra litter decomposition, though biotic changes will likely occur more slowly and lag behind warming[15,50].

We found positive linear relationships between decomposition, soil temperature and soil moisture, with the greatest decomposition occurring in warmer and wetter sites (Fig. 3, Fig. S9). Our 330 study sites encompass the linear range of global biogeochemical modelled relationships of temperature and decomposition, but the non-linear range of soil moisture (Fig. 1, [21]). Thus, our findings indicate that soil moisture may play a key role in mediating the effects of warming on litter decomposition across the temperature-limited tundra biome. Based on these relationships, we estimate that predicted Arctic warming of 2 to 10°C over the 21st century could double summer litter mass loss at the coldest tundra sites. However, changes are highly contingent upon site-specific factors, including moisture availability, substrate quality and decomposer community[15,24,25,27–30,44,52,53]. Although we focus on short-term decomposition processes, greater early-stage decomposition could accelerate biogeochemical cycling[54] and stimulate the loss of older organic carbon[16,55] through nitrogen mining[56–58] or priming of microbial communities[23,59,60].

Contrary to the relationships assumed in many Earth system models[21], we observed neither an exponential increase in decomposition with temperature[20], nor a decrease in decomposition at the highest moisture values (Fig. 3). However, we observed considerable within-site variation in decomposition, emphasising the importance of site-specific factors[52] such as microbial community[61] and soil chemistry[62]. We explored the site-level relationships with general additive models as well as polynomial Bayesian models, and found that overall relationships between environmental variables and decomposition were best fit by linear relationships across variation in temperature and soil moisture (Figs.S2 and S8). However, we did find that for the Eastern Hemisphere, there was an exponential relationship between mass loss and soil moisture driven by data from Svalbard (Figs.S2 and Fig. S8). Overall, our findings could indicate that decomposition is underestimated at colder or wetter tundra sites, but overestimated at warmer sites in current model simulations.

Discrepancy between field observations and modelled decomposition could be caused by environmental interactions. Environmental drivers such as warming and freeze-thaw

11

dynamics may have different influences across the year [35]. With warming, higher temperatures dry surface soils and reduce decomposer activity[63], as has been observed in warming experiments[17,64] and long-term monitoring[65]. Biotic changes to either plant[15,27,29] or decomposer communities[57,66,67] may also respond in complex ways to environmental change. In addition, spatial patterning of landforms and environmental change such as permafrost thaw can create wetter and drier microclimates within the same landscapes that can alter decomposition across scales[44,46,68]. Accounting for real-world biotic and abiotic patterns and interactions among the drivers of decomposition in Earth system models will be critical to more accurately projecting the effects of warming on decomposition and resulting losses to carbon stores[18,20,21,63].

Our tundra-wide decomposition experiment has a number of caveats. Green and rooibos tea are not tundra plant species, but they do encompass the decomposability of tundra plant species (Fig. 2, Fig. S1) and thus provide an excellent common substrate for decomposition studies. Although tea undergoes leaching processes, losing mass due to the loss of water-soluble compounds during *in situ* decomposition[69], so too do tundra plants[41]. We tested leaching rates in our study, finding ~20% greater mass loss for green tea and ~7% greater mass loss for rooibos tea in two-month incubations rather than in 24-hour incubations in liquid water. We found no substantial difference in mass loss with replacement of water across incubations (Fig. S11), suggesting that leaching processes with lateral water flow is likely not a major driver of mass loss in Tea Bag Index studies. Our study only encompasses short-term decomposition with incubation lengths from three months to two years. Litter quality may have a weaker effect on decomposition over longer time periods, and climate or other environmental influences may become stronger over time[70–73].

We used gridded climate data for our tundra-wide extrapolation and for climate data at sites where *in situ* measurements were not recorded. Gridded climate data at high latitudes are extrapolated from more limited meteorological data than at lower latitudes, and at high latitudes, precipitation data are particularly limited[74]. Thus, extrapolations of our statistical results across the tundra biome contain substantial inherent uncertainty (Fig. 5). Our results suggest that decomposition can nonetheless be mapped across large scales[75], and potentially facilitate prediction of decomposition under future climatic conditions. Surprisingly, relationships fitted with *in situ* or the corresponding gridded data displayed consistent trends (Figs. 3, S3-7) although gridded data displayed steeper curves. This suggests that gridded data are fit to represents macroclimatic control over decomposition but could lead to overestimations of decomposition under future climatic condition. An open question is how the

333   more nuanced view of decomposition offered by *in situ* data scales up in explaining global
334   patterns of decomposition [76].

335

336   Changing decomposition rates will have profound implications for the global carbon cycle as
337   the climate is warming [2]. Warming-induced acceleration of litter decomposition could greatly
338   increase carbon losses in the tundra and other high-latitude ecosystems[6], which have
339   historically acted as long-term carbon sinks[14,77]. Tundra regions are also predicted to undergo
340   some of the greatest carbon losses over the coming century[4], although predictions are highly
341   sensitive to data availability[5]. Our study provides well-resolved statistical relationships from
342   standardised field observations that can be used to parameterise Earth system models and
343   refine estimates of this critical feedback to the global carbon cycle. Ultimately, our findings
344   indicate that climate change is likely to increase decomposition across the tundra biome, but
345   that warming-induced vegetation change could have even more pronounced repercussions
346   for this globally important high-latitude carbon store.

347

348   **Methods**
349   We buried 5647 tea bags *in situ* at 5-8 cm depth at 330 sites across the tundra biome (Fig. 2,
350   Table S1). Our database has a hierarchical structure with plots (geographic areas including
351   multiple tea bag incubations) within sites (unique grid referenced locations of multiple plots)
352   within grid cells (the pixels of the gridded climate data, Table S1).

353

354   We recovered tea after three- (summer), nine- (winter), twelve-month (year) and two-year
355   incubations and calculated three metrics of decomposition: (1) percent mass loss, indicating
356   the proportion of initial mass decomposed, (2) stabilisation factor (*S*), indicating the proportion
357   of labile material remaining when initial decomposition has stabilised, and thus long-term
358   carbon storage potential and (3) decomposition rate (*k*), indicating the rate at which labile
359   material is lost, and thus short-term turnover[19]. We removed tea bags with experimental
360   treatments, that increased in mass due to fungal growth, got lost, split during extraction, where
361   labels were no longer legible or when only one site or plot was included per grid cell, resulting
362   in a sample size of 3717 tea bags in the final analysed dataset.

363

364   We examined relationships among the three decomposition metrics, three locally-measured
365   environmental variables (air temperature, soil temperature and soil moisture), and three
366   gridded climate variables: air temperature and precipitation from Climatologies at High
367   Resolution for the Earth's Land Surface (CHELSA)[78] and European Space Agency (ESA) soil
368   moisture data[79] using hierarchical Bayesian models. We also modelled decomposition across
369   tundra and sub-Arctic regions[47] by extrapolating relationships using CHELSA and ESA soil

370   moisture data from 1979 to 2013.

371

372   ***Site Descriptions***

373   We established 330 decomposition sites encompassing 26 geographic regions across the

374   circum-Arctic and alpine tundra (Table S1). Mean annual air temperatures ranged from -

375   10.2°C to 12.7°C, with mean summer temperatures of 24.9°C at the warmest site (Alpine

376   Japan, Site SSJ) and 3.3°C at the coldest site (Svalbard, Endalen Cassiope heath). Sites were

377   largely above treeline though some subarctic and alpine sites extended below treeline.

378
379   ***Decomposition experiment***

380   We measured decomposition using two types of tea in woven nylon mesh bags – a labile

381   green tea and a recalcitrant rooibos tea – following the Tea Bag Index method[19]. The two tea

382   types represent dried leaves of two shrub species (*Camellia sinensis* – green tea and

383   *Aspalathus linearis* – rooibos tea), which strongly differ in their leaf structural and chemical

384   traits[19,80,81]. Although these two species are not native to the tundra, their mass losses are

385   comparable with a range of tundra species (Fig. 2), and allow comparison across sites

386   globally[19,82]. Mass loss via leaching of these tea bags is also comparable with previous studies

387   employing the common litter bag method (24-hour mass loss: 14% for rooibos tea and 37%

388   for green tea, compared to 8 - 32% in litter leaching studies[83]).

389

390   We buried tea bags *in situ* at 5-8 cm depth during 2015-2017. We incubated tea for three

391   approximate time periods – three months (summer: on average 81 days across all sites from

392   late spring – late summer), nine months (winter: late summer to late spring) and twelve months

393   (year: late spring to late spring). Due to the logistical constraints of accessing some field sites,

394   not all incubations were carried out at all sites. We buried a minimum of three tea bag pairwise

395   replicates at each site for each given period. Tea bags were buried, rather than placed on the

396   surface, for consistency with the global standardised Tea Bag Index protocol[19]. Moreover, this

397   increased the likelihood of recovery across the time periods covered in this study. Surface

398   litter likely undergo greater fluctuations in temperature and moisture that may reduce

399   decomposition[83]. Within a common site, we found that annual mass loss was greater for buried

400   teabags compared to those in the litter layer for green tea, but not rooibos tea (Fig. S12).

401   However, litter is commonly mixed into tundra soils through cryoturbation processes[23]. Thus,

402   using a buried litter substrate serves as a proxy for both leaf litter decomposition when

403   incorporated into the soil and soil organic matter decomposition[84].

404

405   We weighed tea bags prior to burial, including both the bag and tag. Upon recovery, we dried

406   bags at 70°C for at least 48 hours, removed any attached soil or roots, and reweighed tea

14

407   bags. We subtracted the mass of the bag and label to determine the mass of the tea only, and

408   the initial masses were corrected to account for initial moisture and loss of material in transit

409   to field sites (approximately 5.6±0.8% of mass for rooibos tea and 3.8 ± 0.4% for green tea,

410   measured using 10 unused tea bags at three different field sites).

411

412   ***Decomposition variables***

413   We calculated three metrics of decomposition: (1) overall mass loss (final tea mass divided by

414   initial tea mass) for each tea type.

415

416   *Equation 1:*

417
$$mass\ loss = 1 - \left(\frac{M_t}{M_0}\right)$$

418   where M_t is equal to the mass of tea at time point t (days) and M_0 is the initial mass.

419

420   (2) The stabilisation factor (*S*), which describes the proportion of potentially decomposable

421   compounds (the hydrolysable or acid-digestible fraction, *H*) remaining upon stabilisation of

422   decomposition. *S* is calculated using green tea, for which mass loss has stabilised within three

423   months of burial[19] (Fig. S10), whereby:

424

425   *Equation 2:*

426
$$S = 1 - \left(\frac{a_g}{H_g}\right)$$

427

428   where a_g is the decomposable fraction (mass loss) of green tea and H_g is the hydrolysable

429   fraction of green tea.

430

431   (3) The decomposition rate (*k*), which represents the rate at which decomposable compounds

432   are lost during decomposition. This two-pool decomposition constant was calculated based

433   on the methods outlined in Keuskamp et al. (2013), and is calculated using rooibos tea, for

434   which decomposition has not yet stabilised during the incubation periods covered by this

435   analysis[19] (Fig. S10).

436

437   *Equation 3:*

438
$$k = ln\left(\frac{a_r}{M_{t(r)} - a_r}\right) x \frac{1}{t}$$

439 where M is equal to the mass of rooibos tea at time point t (days) and a_r is the decomposable

440 fraction of rooibos tea. a_r is calculated from the hydrolysable fraction of rooibos tea (Hr) and

441 stabilisation factor (S), whereby $a_r = H_r (1 - S)$.

442

Environmental variables

444 Where possible, we measured local environmental variables at each site for the duration of

445 the incubation period. Soil temperatures were measured using digital iButtons (DS1921G

446 Thermochron iButtons, Maxim Integrated, San Jose, CA, US) or data loggers (HOBO RX3000

447 Remote Monitoring Station Data Logger, Onset Computer Corporation, Pocasset, MA; HOBO

448 Pendant temperature and light data loggers, Part # UA-002-64, Onset Computer Corporation,

449 Pocasset, MA; Lascar EL USB-1 temperature loggers, Lascar electronics, Salisbury, UK;

450 Theta Probe ML3 attached to a HH2 Moisture Meter Logger, DELTA-T-DEVICES, Cambridge,

451 UK). Soil moisture (percent volumetric water content) was measured using hand-held moisture

452 probes (Spectrum (SM100); HydroSense II; Stevens POGO probe, Stevens Water Monitoring

453 Systems Inc., Portland, OR, USA) at 5 cm depth. Where site-measured data were not

454 available, notably for air temperature, we used local weather station data, provided either by

455 the authors or additional contributors[85] and unpublished data (Annika Kristoffersson pers.

456 comm. 2017, Phil Marsh, pers. comm. 2017). All environmental data were trimmed to the

457 corresponding incubation period for analyses. Sites that did not have available local

458 environmental data were excluded from relevant analyses.

459

Gridded climate variables

461 We used 'Climatologies at high resolution for the Earth's land surface areas' data (CHELSA,

462 0.0083×0.0083 degree resolution[78], http://chelsa-climate.org) to provide gridded temperature

463 and precipitation data for all sites, and to extrapolate decomposition across the tundra biome.

464 We extracted climatologies (covering the time period 1979 to 2013) for summer (June-July-

465 August), winter (December-January-February) and annual temperature and precipitation. We

466 used European Space Agency (ESA) Climate Change Initiative combined soil moisture data

467 product (0.25×0.25-degree resolution[79], https://www.esa-soilmoisture-cci.org) to provide

468 modelled soil moisture for all sites and to extrapolate decomposition across the tundra. We

469 used daily data for the period 1979 to 2013 to build climatologies (summer, winter, year) to

470 align with CHELSA data.

471

472 We compared site-measured environmental data to gridded climate data using hierarchical

473 Bayesian models with grid cell and site as nested random effects using the R package

474 *MCMCglmm*[86] (Fig. 3, Figs. S2-S7 and S9). Site-measured temperature variables correlated

475 closely with gridded temperature data, exhibiting a near 1:1 relationship (Fig. S13). Site-
476 measured moisture was not correlated with average ESA soil moisture data or long-term
477 CHELSA precipitation data (Fig. S13). This discrepancy may result from greater spatial and
478 inter-annual variability in moisture or precipitation compared to temperature[87], or high within-
479 site variation in soil moisture that is not captured by spatially variable and data-poor high-
480 latitude precipitation records at the grid cell scale.
481
Environmental Relationships

483 We conducted three analyses of the relationships among decomposition metrics and
484 environmental variables: (i) relationships between each individual decomposition metric and
485 each environmental variable across all sites (Fig. 3, Figs. S3-S6), (ii) relationships between
486 mass loss and environmental variables within each grid cell (Fig. S7) and (iii) relationships
487 between mass loss and environmental variables accounting for interactions between
488 temperature and moisture (Fig. S9).
489
490 Analyses of environmental relationships were conducted in the statistical programming
491 language *Stan* run through R (v. 3.3.3 to 4.2.3) using packages *rjags*[88] (v. 4.6) and *rstan*[89] (v.
492 2.17.3). In all cases, models were run until convergence was reached, which was assessed
493 both visually in trace plots and by ensuring that all Gelman–Rubin convergence diagnostic
494 values ($\hat{R}$)[90] were less than 1.1. Code is available at:
495 https://github.com/ShrubHub/TundraTeaHub
496
Environmental Relationships – individual variables

498 The relationship between each decomposition metric (decomp) and environmental variable
499 (EV) was estimated from a hierarchical Bayesian model, with climatic variables as the
500 predictor variable and decomposition as the predictor variable, with grid cell (g), site (s, unique
501 grid referenced location) and plot (p, replicate plots within each location) as random effects,
502 varying by tea type (t):
503
Equation 4:

$$decomp_{p,t} \sim Normal\left(\alpha_{p,t} + \alpha_{s,t} + \alpha_{g,t}, \sigma\right)$$

507 We estimated relationships with decomposition metrics over space at the level at which
508 environmental variables were measured, including incubation length (days) as a fixed effect.
509 For example, relationships for gridded climate data were estimated at the level of the grid cell
510 (g), with site (s) and plot (p) as nested hierarchical random effects. Relationships for site-

measured variables were estimated at the site level, with plot (p) as a random effect. If environmental variables were measured at the plot level, we summarised variables to the site level and carried forward the standard deviation among plots into models. If there was only one teabag per plot, one plot per site or one site per grid cell, $\alpha_{p,t}$ or $\alpha_{s,t}$ was set to zero. Note that data availability differs for each environmental variable. For stabilisation factor (S) and decomposition rate (k) models, we did not vary effects by tea type (t), since only one tea type is used for each of these variables.

Equation 5:

$$\alpha_{g,t} \sim Normal(\gamma 0_t + \gamma 1_t * EV_{g,t} + \gamma 2_t * days_{g,t}, \theta)$$

$$\alpha_{p,t} \sim Normal(0, \sigma 1)$$

$$\alpha_{s,t} \sim Normal(0, \sigma 2)$$

We modelled all incubation periods separately due to large differences in the availability of environmental data and qualitative differences between conditions in different seasons such as frozen ground during the winter.

Decomposition relationship with temperature and moisture can also be exponential, saturating or sigmoidal [22,91,92]. To account for this, we also tested a potential non-linear relationship between summer mass loss and the environmental variables by including a fourth fixed parameter in equation 5, multiplying the square of the environmental variable, hence allowing the relationship to be polynomial.

Environmental Relationships – within grid cells
We modelled the relationship between decomposition metrics and environmental variables (single variables only) within grid cells using the same model structure, but by standardising all environmental variables within a grid cell using mean zero and unit-variance scaling.

Environmental Relationships – temperature and moisture interactions
We modelled the relationships between mass loss and environmental variables over space accounting for both temperature and moisture within the same model (both for site-measured soil temperature and soil moisture, and for gridded air temperature and soil moisture). We used the same model structure as for individual variables, but also included an interaction term between these two environmental variables.

Equation 6:

547 $$\alpha_{g,t} \sim Normal(\gamma0_t + \gamma1_t * temp_{g,t} + \gamma2_t * moisture_{g,t} + \gamma3_t * temp_{g,t} * moisture_{g,t} + \gamma4_t$$

548 $$* days_{g,t}, \theta)$$

549

550 We ran models with environmental data in original units, and also using standardised

551 environmental variables and incubation length using mean zero and unit-variance scaling to

552 allow comparison across environmental variables.

553

554 ***Mapping decomposition***

555 We used model estimates from the gridded climate variable model (Equation 6) to map

556 decomposition over space based on summer temperature and moisture for tundra and

557 subarctic climate regions. We mapped gridded temperature of the warmest quarter (CHELSA

558 bio10) and gridded summer soil moisture (ESA, June-July-August) as environmental

559 variables. We used the coefficients for green tea (Fig. 5) and rooibos tea (Fig. S14), and

560 assumed the mean incubation length across summer treatments (81 days). We masked

561 estimates to tundra and subarctic climate regions based on the Köppen-Geiger climate

562 classification[93] (regions ET, Dsc, Dsc, Dwc, Dwd, Dfc, Dfd). We included an estimation of

563 global treeline based on the Circum-Arctic Vegetation Map (CAVM) classification[48].

19

References

564

565   1. Bond-Lamberty, B. & Thomson, A. Temperature-associated increases in the global soil
566   respiration record. *Nature* **464**, 579–582 (2010).

567   2. Davidson, E. A. & Janssens, I. A. Temperature sensitivity of soil carbon decomposition
568   and feedbacks to climate change. *Nature* **440**, 165–173 (2006).

569   3. Conant, R. T. *et al.* Temperature and soil organic matter decomposition rates –
570   synthesis of current knowledge and a way forward. *Glob. Change Biol.* **17**, 3392–3404
571   (2011).

572   4. Crowther, T. W. *et al.* Quantifying global soil carbon losses in response to warming.
573   *Nature* **540**, 104–108 (2016).

574   5. van Gestel, N. *et al.* Predicting soil carbon loss with warming. *Nature* **554**, E4–E5
575   (2018).

576   6. Wieder, W. R., Sulman, B. N., Hartman, M. D., Koven, C. D. & Bradford, M. A. Arctic Soil
577   Governs Whether Climate Change Drives Global Losses or Gains in Soil Carbon.
578   *Geophys. Res. Lett.* **46**, 14486–14495 (2019).

579   7. Hugelius, G. *et al.* The Northern Circumpolar Soil Carbon Database: spatially distributed
580   datasets of soil coverage and soil carbon storage in the northern permafrost regions.
581   *Earth Syst. Sci. Data* **5**, 3–13 (2013).

582   8. Tarnocai, C. *et al.* Soil organic carbon pools in the northern circumpolar permafrost
583   region. *Glob. Biogeochem. Cycles* **23**, (2009).

584   9. Mishra, U. *et al.* Spatial heterogeneity and environmental predictors of permafrost region
585   soil organic carbon stocks. *Sci. Adv.* **7**, eaaz5236 (2021).

586 10. Schuur, E. A. G. *et al.* The effect of permafrost thaw on old carbon release and net
587   carbon exchange from tundra. *Nature* **459**, 556–559 (2009).

588 11. Aerts, R. The freezer defrosting: global warming and litter decomposition rates in cold
589   biomes. *J. Ecol.* **94**, 713–724 (2006).

590 12. Rantanen, M. *et al.* The Arctic has warmed nearly four times faster than the globe since
591   1979. *Commun. Earth Environ.* **3**, 1–10 (2022).

592 13. IPCC Working Group I. *Climate Change 2021: The Physical Science Basis. Contribution*
593   *of Working Group I to the Sixth Assessment Report of the Intergovernmental Panel on*
594   *Climate Change*. https://www.ipcc.ch/report/ar6/wg1/ (2021).

595 14. Schuur, E. A. G. *et al.* Climate change and the permafrost carbon feedback. *Nature* **520**,
596   171–179 (2015).

597 15. Björnsdóttir, K., Barrio, I. C. & Jónsdóttir, I. S. Long-term warming manipulations reveal
598   complex decomposition responses across different tundra vegetation types. *Arct. Sci.* 1–
599   13 (2021) doi:10.1139/as-2020-0046.

600   16. Cornelissen, J. H. C. *et al.* Global negative vegetation feedback to climate warming
601   responses of leaf litter decomposition rates in cold biomes. *Ecol. Lett.* **10**, 619–627
602   (2007).

603   17. Christiansen, C. T. *et al.* Enhanced summer warming reduces fungal decomposer
604   diversity and litter mass loss more strongly in dry than in wet tundra. *Glob. Change Biol.*
605   **23**, 406–420 (2017).

606   18. Hicks Pries, C. E., Schuur, E. A. G., Vogel, J. G. & Natali, S. M. Moisture drives surface
607   decomposition in thawing tundra. *J. Geophys. Res. Biogeosciences* **118**, 1133–1143
608   (2013).

609   19. Keuskamp, J. A., Dingemans, B. J. J., Lehtinen, T., Sarneel, J. M. & Hefting, M. M. Tea
610   Bag Index: a novel approach to collect uniform decomposition data across ecosystems.
611   *Methods Ecol. Evol.* **4**, 1070–1075 (2013).

612   20. Liski, J., Nissinen, A., Erhard, M. & Taskinen, O. Climatic effects on litter decomposition
613   from arctic tundra to tropical rainforest. *Glob. Change Biol.* **9**, 575–584 (2003).

614   21. Sierra, C. A., Trumbore, S. E., Davidson, E. A., Vicca, S. & Janssens, I. Sensitivity of
615   decomposition rates of soil organic matter with respect to simultaneous changes in
616   temperature and moisture. *J. Adv. Model. Earth Syst.* **7**, 335–356 (2015).

617   22. Bonan, G. B., Hartman, M. D., Parton, W. J. & Wieder, W. R. Evaluating litter
618   decomposition in earth system models with long-term litterbag experiments: an example
619   using the Community Land Model version 4 (CLM4). *Glob. Change Biol.* **19**, 957–974
620   (2013).

621   23. Sistla, S. A. *et al.* Long-term warming restructures Arctic tundra without changing net soil
622   carbon storage. *Nature* **497**, 615–618 (2013).

623   24. Christiansen, C. T., Mack, M. C., DeMarco, J. & Grogan, P. Decomposition of Senesced
624   Leaf Litter is Faster in Tall Compared to Low Birch Shrub Tundra. *Ecosystems* **21**,
625   1564–1579 (2018).

626   25. Cornwell, W. K. *et al.* Plant species traits are the predominant control on litter
627   decomposition rates within biomes worldwide. *Ecol. Lett.* **11**, 1065–1071 (2008).

628   26. Hobbie, S. E. Temperature and plant species control over litter decomposition in Alaskan
629   tundra. *Ecol. Monogr.* **66**, 503–522 (1996).

630   27. Parker, T. C. *et al.* Exploring drivers of litter decomposition in a greening Arctic: results
631   from a transplant experiment across a treeline. *Ecology* **99**, 2284–2294 (2018).

632   28. Petraglia, A. *et al.* Litter decomposition: effects of temperature driven by soil moisture
633   and vegetation type. *Plant Soil* **435**, 187–200 (2019).

634   29. Fanin, N. *et al.* Relative Importance of Climate, Soil and Plant Functional Traits During
635   the Early Decomposition Stage of Standardized Litter. *Ecosystems* **23**, 1004–1018
636   (2020).

637 30. Joly, F.-X., Scherer-Lorenzen, M. & Hättenschwiler, S. Resolving the intricate role of
638   climate in litter decomposition. *Nat. Ecol. Evol.* **7**, 214–223 (2023).

639 31. Elmendorf, S. C. *et al.* Plot-scale evidence of tundra vegetation change and links to
640   recent summer warming. *Nat. Clim. Change* **2**, 453–457 (2012).

641 32. García Criado, M. *et al.* Plant diversity dynamics over space and time in a warming
642   Arctic. *Nature* 1–9 (2025) doi:10.1038/s41586-025-08946-8.

643 33. García Criado, M., Myers-Smith, I. H., Bjorkman, A. D., Lehmann, C. E. R. & Stevens, N.
644   Woody plant encroachment intensifies under climate change across tundra and savanna
645   biomes. *Glob. Ecol. Biogeogr.* **29**, 925–943 (2020).

646 34. Myers-Smith, I. H. *et al.* Shrub expansion in tundra ecosystems: dynamics, impacts and
647   research priorities. *Environ. Res. Lett.* **6**, 045509 (2011).

648 35. Blok, D., Elberling, B. & Michelsen, A. Initial Stages of Tundra Shrub Litter
649   Decomposition May Be Accelerated by Deeper Winter Snow But Slowed Down by
650   Spring Warming. *Ecosystems* **19**, 155–169 (2016).

651 36. Carbognani, M., Petraglia, A. & Tomaselli, M. Warming effects and plant trait control on
652   the early-decomposition in alpine snowbeds. *Plant Soil* **376**, 277–290 (2014).

653 37. García-Palacios, P., Maestre, F. T., Kattge, J. & Wall, D. H. Climate and litter quality
654   differently modulate the effects of soil fauna on litter decomposition across biomes. *Ecol.*
655   *Lett.* **16**, 1045–1053 (2013).

656 38. Moore, T. R., Trofymow, J. A., Prescott, C. E., Fyles, J. & Titus, B. D. Patterns of
657   Carbon, Nitrogen and Phosphorus Dynamics in Decomposing Foliar Litter in Canadian
658   Forests. *Ecosystems* **9**, 46–62 (2006).

659 39. Zhang, D., Hui, D., Luo, Y. & Zhou, G. Rates of litter decomposition in terrestrial
660   ecosystems: global patterns and controlling factors. *J. Plant Ecol.* **1**, 85–93 (2008).

661 40. Duddigan, S., Shaw, L. J., Alexander, P. D. & Collins, C. D. Chemical Underpinning of
662   the Tea Bag Index: An Examination of the Decomposition of Tea Leaves. *Appl. Environ.*
663   *Soil Sci.* **2020**, 6085180 (2020).

664 41. Blume-Werry, G. *et al.* Don't drink it, bury it: comparing decomposition rates with the tea
665   bag index is possible without prior leaching. *Plant Soil* **465**, 613–621 (2021).

666 42. Mori, T. Tea Bag Index Revisited: Risks of Misleading Decomposition Patterns. *Ecol.*
667   *Lett.* **28**, e70010 (2025).

668 43. Sarneel, J. M. *et al.* The Assumptions of the Tea Bag Index and Their Implications: A
669   Reply to Mori 2025. *Ecol. Lett.* **28**, e70117 (2025).

670 44. Gallois, E. *et al.* Litter decomposition is moderated by scale-dependent
671   microenvironmental variation in tundra ecosystems. Preprint at
672   https://doi.org/10.32942/osf.io/crup3 (2022).

673 45. von Oppen, J. *et al.* Microclimate explains little variation in year-round decomposition
674   across an Arctic tundra landscape. In: Arctic shrubs between macro- and microclimate:
675   lessons across scales from Western Greenland. (Aarhus University, Aarhus, Denmark,
676   2022).

677 46. Walker, E. R., Haydn J. D. Thomas, & Isla H. Myers-Smith. Experimental evidence of
678   litter quality and soil moisture rather than temperature as the key driver of litter
679   decomposition along a high-latitude elevational gradient. Preprint at
680   https://doi.org/10.32942/X2M880 (2023).

681 47. Kottek, M., Grieser, J., Beck, C., Rudolf, B. & Rubel, F. World map of the Köppen-Geiger
682   climate classification updated. *Meteorol. Z.* **15**, 259–263 (2006).

683 48. Walker, D. A. *et al.* The Circumpolar Arctic vegetation map. *J. Veg. Sci.* **16**, 267–282
684   (2005).

685 49. Sarneel, J. M. *et al.* Reading tea leaves worldwide: Decoupled drivers of initial litter
686   decomposition mass-loss rate and stabilization. *Ecol. Lett.* **27**, e14415 (2024).

687 50. Bjorkman, A. D. *et al.* Plant functional trait change across a warming tundra biome.
688   *Nature* **562**, 57–62 (2018).

689 51. Bjorkman, A. D. *et al.* Status and trends in Arctic vegetation: Evidence from experimental
690   warming and long-term monitoring. *Ambio* **49**, 678–692 (2020).

691 52. Bradford, M. A. *et al.* Climate fails to predict wood decomposition at regional scales. *Nat.*
692   *Clim. Change* **4**, 625–630 (2014).

693 53. McLaren, J. R. *et al.* Shrub encroachment in Arctic tundra: Betula nana effects on
694   above- and belowground litter decomposition. *Ecology* **98**, 1361–1376 (2017).

695 54. Buckeridge, K. M., Zufelt, E., Chu, H. & Grogan, P. Soil nitrogen cycling rates in low
696   arctic shrub tundra are enhanced by litter feedbacks. *Plant Soil* **330**, 407–421 (2010).

697 55. Mack, M. C., Schuur, E. A. G., Bret-Harte, M. S., Shaver, G. R. & Chapin, F. S.
698   Ecosystem carbon storage in Arctic tundra reduced by long-term nutrient fertilization.
699   *Nature* **431**, 440–443 (2004).

700 56. Clemmensen, K. E. *et al.* A tipping point in carbon storage when forest expands into
701   tundra is related to mycorrhizal recycling of nitrogen. *Ecol. Lett.* **24**, 1193–1204 (2021).

702 57. Hicks, L. C., Yuan, M., Brangarí, A., Rousk, K. & Rousk, J. Increased Above- and
703   Belowground Plant Input Can Both Trigger Microbial Nitrogen Mining in Subarctic
704   Tundra Soils. *Ecosystems* **25**, 105–121 (2022).

705 58. Moorhead, D. L. & Sinsabaugh, R. L. A Theoretical Model of Litter Decay and Microbial
706   Interaction. *Ecol. Monogr.* **76**, 151–174 (2006).

707 59. Keuper, F. *et al.* Carbon loss from northern circumpolar permafrost soils amplified by
708   rhizosphere priming. *Nat. Geosci.* **13**, 560–565 (2020).

709 60. Street, L. E. *et al.* Plant carbon allocation drives turnover of old soil organic matter in
710 permafrost tundra soils. *Glob. Change Biol.* **26**, 4559–4571 (2020).

711 61. Wardle, D. A. *et al.* Ecological Linkages Between Aboveground and Belowground Biota.
712 *Science* **304**, 1629–1633 (2004).

713 62. Knorr, M., Frey, S. D. & Curtis, P. S. Nitrogen Additions and Litter Decomposition: A
714 Meta-Analysis. *Ecology* **86**, 3252–3257 (2005).

715 63. Thakur, M. P. *et al.* Reduced feeding activity of soil detritivores under warmer and drier
716 conditions. *Nat. Clim. Change* **8**, 75–78 (2018).

717 64. Rinnan, R., Michelsen, A. & Jonasson, S. Effects of litter addition and warming on soil
718 carbon, nutrient pools and microbial communities in a subarctic heath ecosystem. *Appl.*
719 *Soil Ecol.* **39**, 271–281 (2008).

720 65. Koltz, A. M., Schmidt, N. M. & Høye, T. T. Differential arthropod responses to warming
721 are altering the structure of Arctic communities. *R. Soc. Open Sci.* **5**, 171503 (2018).

722 66. Peng, Y. *et al.* Soil fauna effects on litter decomposition are better predicted by fauna
723 communities within litterbags than by ambient soil fauna communities. *Plant Soil* (2023)
724 doi:10.1007/s11104-023-05902-1.

725 67. Xue, K. *et al.* Tundra soil carbon is vulnerable to rapid microbial decomposition under
726 climate warming. *Nat. Clim. Change* **6**, 595–600 (2016).

727 68. Lara, M. J. *et al.* Local-scale Arctic tundra heterogeneity affects regional-scale carbon
728 dynamics. *Nat. Commun.* **11**, 4925 (2020).

729 69. Lind, L., Harbicht, A., Bergman, E., Edwartz, J. & Eckstein, R. L. Effects of initial
730 leaching for estimates of mass loss and microbial decomposition—Call for an increased
731 nuance. *Ecol. Evol.* **12**, e9118 (2022).

732 70. Canessa, R. *et al.* Relative effects of climate and litter traits on decomposition change
733 with time, climate and trait variability. *J. Ecol.* **109**, 447–458 (2021).

734 71. Harmon, M. E. *et al.* Long-term patterns of mass loss during the decomposition of leaf
735 and fine root litter: an intersite comparison. *Glob. Change Biol.* **15**, 1320–1338 (2009).

736 72. Hollister, R. D., Webber, P. J. & Tweedie, C. E. The response of Alaskan arctic tundra to
737 experimental warming: differences between short- and long-term responses. *Glob.*
738 *Change Biol.* **11**, 525–536 (2005).

739 73. Trofymow, J. A. *et al.* Rates of litter decomposition over 6 years in Canadian forests:
740 influence of litter quality and climate. *Can. J. For. Res.* **32**, 789–804 (2002).

741 74. Macias-Fauria, M., Seddon, A. W. R., Benz, D., Long, P. R. & Willis, K. Spatiotemporal
742 patterns of warming. *Nat. Clim. Change* **4**, 845–846 (2014).

743 75. Althuizen, I. H. J., Lee, H., Sarneel, J. M. & Vandvik, V. Long-Term Climate Regime
744 Modulates the Impact of Short-Term Climate Variability on Decomposition in Alpine
745 Grassland Soils. *Ecosystems* **21**, 1580–1592 (2018).

746   76. Joly, F.-X., Scherer-Lorenzen, M. & Hättenschwiler, S. Resolving the intricate role of
747   climate in litter decomposition. *Nat. Ecol. Evol.* **7**, 214–223 (2023).

748   77. Virkkala, A.-M. *et al.* Statistical upscaling of ecosystem CO2 fluxes across the terrestrial
749   tundra and boreal domain: Regional patterns and uncertainties. *Glob. Change Biol.* **27**,
750   4040–4059 (2021).

751   78. Karger, D. N. *et al.* Climatologies at high resolution for the earth's land surface areas.
752   *Sci. Data* **4**, 170122 (2017).

753   79. Dorigo, W. *et al.* ESA CCI Soil Moisture for improved Earth system understanding:
754   State-of-the art and future directions. *Remote Sens. Environ.* **203**, 185–215 (2017).

755   80. Graham, H. N. Green tea composition, consumption, and polyphenol chemistry. *Prev.*
756   *Med.* **21**, 334–350 (1992).

757   81. Krafczyk, N. & Glomb, M. A. Characterization of Phenolic Compounds in Rooibos Tea. *J.*
758   *Agric. Food Chem.* **56**, 3368–3376 (2008).

759   82. Djukic, I. *et al.* Early stage litter decomposition across biomes. *Sci. Total Environ.* **628–**
760   **629**, 1369–1394 (2018).

761   83. Bokhorst, S., Bjerke, J. W., Melillo, J., Callaghan, T. V. & Phoenix, G. K. Impacts of
762   extreme winter warming events on litter decomposition in a sub-arctic heathland. *Soil*
763   *Biol. Biochem.* **42**, 611–617 (2010).

764   84. Eskelinen, A., Stark, S. & Männistö, M. Links between plant community composition, soil
765   organic matter quality and microbial communities in contrasting tundra habitats.
766   *Oecologia* **161**, 113–123 (2009).

767   85. Niittynen, P. *et al.* Fine-scale tundra vegetation patterns are strongly related to winter
768   thermal conditions. *Nat. Clim. Change* **10**, 1143–1148 (2020).

769   86. Hadfield, J. D. MCMC Methods for Multi-Response Generalized Linear Mixed Models:
770   The MCMCglmm R Package. **33**, 1–22 (2010).

771   87. Seneviratne, S. I. *et al.* Investigating soil moisture–climate interactions in a changing
772   climate: A review. *Earth-Sci. Rev.* **99**, 125–161 (2010).

773   88. Plummer, M. rjags: Bayesian Graphical Models using MCMC. (2016).

774   89. Stan Development Team. RStan: the R interface to Stan. (2018).

775   90. Gelman, A. & Rubin, D. B. Inference from Iterative Simulation Using Multiple Sequences.
776   *Stat. Sci.* **7**, 457–472 (1992).

777   91. Davidson, E. A. & Janssens, I. A. Temperature sensitivity of soil carbon decomposition
778   and feedbacks to climate change. *Nature* **440**, 165–173 (2006).

779   92. Tuomi, M., Vanhala, P., Karhu, K., Fritze, H. & Liski, J. Heterotrophic soil respiration—
780   Comparison of different models describing its temperature dependence. *Ecol. Model.*
781   **211**, 182–190 (2008).

782   93. Peel, M. C., Finlayson, B. L. & McMahon, T. A. Updated world map of the Köppen-
783   Geiger climate classification. *Hydrol. Earth Syst. Sci.* **11**, 1633–1644 (2007).
784   94. Bjorkman, A. D. *et al.* Tundra Trait Team: A database of plant traits spanning the tundra
785   biome. *Glob. Ecol. Biogeogr.* **27**, 1402–1411 (2018).
786   95. Bjorkman, A. D. *et al.* Plant functional trait change across a warming tundra biome.
787   *Nature* **562**, 57–62 (2018).
788

Supplementary Tables

Table S1. Summary of geographic locations used in main study, indicating number of sites and plots (the base study unit), number of tea bag replicates used in study, and mean temperatures (CHELSA data 1979-2013, summer = warmest quarter, winter = coldest quarter), mean elevation of the sites, and a general description of the sites.

Geographic Region	Number of sites	Number of plots	Number of tea bags	Mean temperature (°C) (year / summer / winter)			Elevation (m a.s.l)	Sites description
Alpine Japan	45	46	776	6.7	18.7	-4.5	1576	Alpine tundra
Auðkúluheiði, Iceland	3	26	110	0.9	8.6	-5.0	486	Subarctic shrub tundra dominated by *Betula nana*
Australian Alps	1	18	191	4.7	11.4	-1.5	1880	Alpine tundra
Disko Island, Greenland	7	7	112	-4.0	7.1	-15.4	8	Prostrate/hemi-prostrate dwarf-shrub, lichen tundra
Fairbanks, Alaska	7	14	56	-4.8	14.3	-22.0	501	Erect dwarf-shrub, moss tundra
Kilpisjärvi, Finland	82	120	751	-2.1	10.2	-13.2	672	Subarctic tundra from birch forest to birch shrubs
Gothic Mountain, Colorado, USA	5	5	95	2.2	13.4	-8.1	2922	Alpine tundra
Italian Alps	2	14	116	-1.6	7.5	-10.1	2569	Alpine tundra dominated by *Salix herbacea* and mosses
Kangerlussuaq, Greenland	2	2	36	-5.6	7.5	-16.6	280	*Salix glauca* and *Betula nana* tundra and steppe tundra
Khanymey, western Siberia	2	2	15	-3.6	15.4	-21.1	66	Subarctic pine and larch forests
Kluane, Yukon, Canada	15	72	757	-3.1	8.8	-14.1	1414	Alpine tundra
Lofoten Islands, Norway	1	16	55	5.8	12.6	0.8	15	Subarctic grass and forb tundra
Narsarsuaq, Greenland	10	49	450	-3.3	6.6	-12.0	207	Prostrate dwarf-shrub, herb, lichen tundra
Northern Norway	35	62	119	0.5	11.9	-9.7	356	Gradient from birch forests to alpine tundra (shrubs, meadows).
Northern Sweden	56	122	467	-2.1	9.9	-12.8	796	Gradient from birch forests to alpine tundra (heathland, shrubs, tundra meadows).
Qikiqtaruk-Herschel Island, Yukon, Canada	9	14	224	-9.4	7.6	-24.3	38	Coastal tundra with shrub, sedge, grass and forb.
Southampton Island, Nunavut, Canada	1	1	5	-9.4	6.4	-26.6	12	Cryptogam, barren complex
Svalbard	25	109	468	-6.3	4.2	-14.7	40	Graminoid, forb, cryptogam tundra and dwarf-shrub, lichen tundra
Swiss Alps	3	61	256	-1.00	8.0	-9.4	2180	Alpine tundra
Þeistareykir, Iceland	2	12	72	1.7	8.9	-3.5	340	Subarctic shrub tundra dominated by *Betula nana*
Þingvellir, Iceland	1	10	40	4.0	10.7	-1.1	120	Subarctic tundra dominated by birch trees and dwarf birches
Tazovsky, western Siberia	1	1	8	-7.4	12.5	-25.1	24	Subarctic shrub tundra with sporadic trees
Toolik Lake, Alaska, USA	2	7	140	-10.2	10.4	-26.6	760	Alpine tundra
Trail Valley, NWT, Canada	10	30	180	-9.1	12.0	-27.2	95	From sporadic boreal tree species to shrub tundra
Umiujaq, Québec, Canada	2	2	40	-3.9	9.9	-20.8	81	Subactic shrub tundra with maritime influence
Urengoy, western Siberia	1	1	8	-6.3	13.7	-24.0	26	Subarctic tundra with sporadic trees

27

Environ. Variable	Decomp. variable	Time period	Tea Type	Parameter	Mean	SD	2.50%	97.50%	Sample size	Effective sample size
Air temp. (measured)	Mass loss	Summer	G	Intercept	0.531	0.006	0.519	0.543	1913	15 000
Air temp. (measured)	Mass loss	Summer	R	Intercept	0.17	0.006	0.158	0.182	1913	15 000
Air temp. (measured)	**Mass loss**	**Summer**	**G**	**Slope**	**0.008**	**0.002**	**0.004**	**0.012**	**1913**	**15 000**
Air temp. (measured)	**Mass loss**	**Summer**	**R**	**Slope**	**0.005**	**0.002**	**0.001**	**0.004**	**1913**	**15 000**
Soil temp. (measured)	Mass loss	Summer	G	Intercept	0.605	0.006	0.593	0.616	1560	15 000
Soil temp. (measured)	Mass loss	Summer	R	Intercept	0.22	0.006	0.208	0.231	1560	15 000
Soil temp. (measured)	**Mass loss**	**Summer**	**G**	**Slope**	**0.02**	**0.002**	**0.017**	**0.023**	**1560**	**15 000**
Soil temp. (measured)	**Mass loss**	**Summer**	**R**	**Slope**	**0.011**	**0.002**	**0.008**	**0.014**	**1560**	**15 000**
Moisture (measured)	Mass loss	Summer	G	Intercept	0.523	0.009	0.504	0.541	917	15 000
Moisture (measured)	Mass loss	Summer	R	Intercept	0.183	0.009	0.165	0.201	917	15 000
Moisture (measured)	**Mass loss**	**Summer**	**G**	**Slope**	**7.36E-04**	**3.75E-04**	**1.45E-05**	**1.47E-03**	**917**	**14 142**
Moisture (measured)	Mass loss	Summer	R	Slope	7.16E-05	3.68E-04	-6.57E-04	8.09E-04	917	15 000
Air temp. (CHELSA)	Mass loss	Summer	G	Intercept	0.559	0.009	0.541	0.577	2837	15 000
Air temp. (CHELSA)	Mass loss	Summer	R	Intercept	0.204	0.009	0.187	0.222	2837	15 000
Air temp. (CHELSA)	**Mass loss**	**Summer**	**G**	**Slope**	**0.017**	**0.002**	**0.013**	**0.021**	**2837**	**7178**
Air temp. (CHELSA)	**Mass loss**	**Summer**	**R**	**Slope**	**0.012**	**0.002**	**0.008**	**0.015**	**2837**	**15 000**
Precip. (CHELSA)	Mass loss	Summer	G	Intercept	0.565	0.01	0.545	0.585	2837	15 000
Precip. (CHELSA)	Mass loss	Summer	R	Intercept	0.209	0.01	0.19	0.229	2837	15 000
Precip. (CHELSA)	**Mass loss**	**Summer**	**G**	**Slope**	**0.004**	**0.001**	**0.003**	**0.005**	**2837**	**15 000**
Precip. (CHELSA)	**Mass loss**	**Summer**	**R**	**Slope**	**0.003**	**0.001**	**0.003**	**0.004**	**2837**	**15 000**
Moisture (ESA)	Mass loss	Summer	G	Intercept	0.595	0.013	0.569	0.621	2234	15 000
Moisture (ESA)	Mass loss	Summer	R	Intercept	0.232	0.013	0.206	0.258	2234	15 000
Moisture (ESA)	**Mass loss**	**Summer**	**G**	**Slope**	**0.013**	**0.004**	**0.005**	**0.02**	**2234**	**15 000**
Moisture (ESA)	Mass loss	Summer	R	Slope	0.007	0.004	-9.38E-05	0.015	2234	15 000
Air temp. (measured)	Mass loss	Winter	G	Intercept	0.561	0.03	0.503	0.621	176	15 000
Air temp. (measured)	Mass loss	Winter	R	Intercept	0.226	0.031	0.165	0.287	176	15 000
Air temp. (measured)	**Mass loss**	**Winter**	**G**	**Slope**	**0.044**	**0.016**	**0.012**	**0.074**	**176**	**15 000**
Air temp. (measured)	Mass loss	Winter	R	Slope	-0.002	0.016	-0.033	0.029	176	15 000
Soil temp. (measured)	Mass loss	Winter	G	Intercept	0.498	0.041	0.416	0.58	71	5842

Soil temp. (measured)	Mass loss	Winter	R	Intercept	0.195	0.113	0.113	0.278	71	15 000
Soil temp. (measured)	Mass loss	Winter	G	Slope	0.003	0.008	-0.013	0.019	71	7964
Soil temp. (measured)	Mass loss	Winter	R	Slope	0.004	0.008	-0.012	0.02	71	15 000
Moisture (measured)	Mass loss	Winter	G	Intercept	0.553	0.007	0.538	0.567	206	9488
Moisture (measured)	Mass loss	Winter	R	Intercept	0.19	0.007	0.175	0.204	206	8980
Moisture (measured)	Mass loss	Winter	G	Slope	0.001	0.001	-1.51E-05	0.002	206	12 291
Moisture (measured)	Mass loss	Winter	R	Slope	4.42E-04	0.001	-5.93E-04	0.001	206	15 000
Air temp. (CHELSA)	Mass loss	Winter	G	Intercept	0.542	0.005	0.451	0.637	427	15 000
Air temp. (CHELSA)	Mass loss	Winter	R	Intercept	0.208	0.005	0.116	0.3	427	15 000
Air temp. (CHELSA)	Mass loss	Winter	G	Slope	0.019	0.012	-0.006	0.043	427	15 000
Air temp. (CHELSA)	Mass loss	Winter	R	Slope	-3.47E-05	0.012	-0.024	0.024	427	15 000
Precip. (CHELSA)	Mass loss	Winter	G	Intercept	0.54	0.046	0.453	0.634	427	15 000
Precip. (CHELSA)	Mass loss	Winter	R	Intercept	0.206	0.046	0.114	0.299	427	15 000
Precip. (CHELSA)	Mass loss	Winter	G	Slope	0.005	0.003	-0.001	0.011	427	15 000
Precip. (CHELSA)	Mass loss	Winter	R	Slope	-4.88E-04	0.003	-0.007	0.006	427	15 000
Moisture (ESA)	Mass loss	Winter	G	Intercept	0.541	0.045	0.451	0.633	309	15 000
Moisture (ESA)	Mass loss	Winter	R	Intercept	0.207	0.046	0.118	0.298	309	15 000
Moisture (ESA)	**Mass loss**	**Winter**	**G**	**Slope**	**0.073**	**0.032**	**0.008**	**0.137**	**309**	**15 000**
Moisture (ESA)	Mass loss	Winter	R	Slope	-0.01	0.033	-0.075	0.054	309	15 000
Air temp. (measured)	Mass loss	Year	G	Intercept	0.581	0.006	0.578	0.6	1251	15 000
Air temp. (measured)	Mass loss	Year	R	Intercept	0.228	0.006	0.217	0.24	1251	15 000
Air temp. (measured)	**Mass loss**	**Year**	**G**	**Slope**	**0.011**	**0.002**	**0.007**	**0.015**	**1251**	**15 000**
Air temp. (measured)	**Mass loss**	**Year**	**R**	**Slope**	**0.014**	**0.002**	**0.01**	**0.018**	**1251**	**15 000**
Soil temp. (measured)	Mass loss	Year	G	Intercept	0.591	0.014	0.564	0.619	342	15 000
Soil temp. (measured)	Mass loss	Year	R	Intercept	0.263	0.014	0.237	0.29	342	15 000
Soil temp. (measured)	**Mass loss**	**Year**	**G**	**Slope**	**0.018**	**0.004**	**0.011**	**0.027**	**342**	**15 000**
Soil temp. (measured)	**Mass loss**	**Year**	**R**	**Slope**	**0.019**	**0.004**	**0.011**	**0.027**	**342**	**15 000**
Moisture (measured)	Mass loss	Year	G	Intercept	0.614	0.005	0.604	0.625	760	15 000
Moisture (measured)	Mass loss	Year	R	Intercept	0.255	0.006	0.245	0.266	760	15 000
Moisture (measured)	Mass loss	Year	G	Slope	-0.001	3.89E-04	-0.001	1.54E-04	760	15 000
Moisture (measured)	Mass loss	Year	R	**Slope**	**-0.001**	**4.06E-04**	**-0.002**	**1.06E-04**	**760**	**15 000**
Air temp. (CHELSA)	Mass loss	Year	G	Intercept	0.606	0.011	0.585	0.628	1377	15 000
Air temp. (CHELSA)	Mass loss	Year	R	Intercept	0.236	0.011	0.215	0.258	1377	15 000
Air temp. (CHELSA)	**Mass loss**	**Year**	**G**	**Slope**	**0.015**	**0.003**	**0.009**	**0.02**	**1377**	**10 775**
Air temp. (CHELSA)	**Mass loss**	**Year**	**R**	**Slope**	**0.01**	**0.003**	**0.004**	**0.015**	**1377**	**9975**

29

Precip. (CHELSA)	Mass loss	Year	G	Intercept	0.601	0.015	0.572	0.631	1377	15 000
Precip. (CHELSA)	Mass loss	Year	R	Intercept	0.236	0.015	0.207	0.265	1377	15 000
Precip. (CHELSA)	**Mass loss**	**Year**	**G**	**Slope**	**0.001**	**4.15E-04**	**2.48E-04**	**0.002**	**1377**	**15 000**
Precip. (CHELSA)	Mass loss	Year	R	Slope	3.06E-04	4.05E-04	-5.02E-04	0.001	1377	15 000
Moisture (ESA)	Mass loss	Year	G	Intercept	0.62	0.017	0.588	0.655	1098	15 000
Moisture (ESA)	Mass loss	Year	R	Intercept	0.252	0.017	0.219	0.285	1098	15 000
Moisture (ESA)	Mass loss	Year	G	Slope	0.008	0.004	-4.67E-05	0.015	1098	15 000
Moisture (ESA)	Mass loss	Year	R	Slope	0.005	0.004	-2.84E-03	0.007	1098	15 000
Air temp. (measured)	k	Summer	R	Intercept	0.011	3.89E-04	0.01	0.012	927	15 000
Air temp. (measured)	**k**	**Summer**	**R**	**Slope**	**4.28E-04**	**1.36E-04**	**1.59E-04**	**6.97E-04**	**927**	**15 000**
Soil temp. (measured)	k	Summer	R	Intercept	0.011	3.29E-04	0.01	0.011	704	15 000
Soil temp. (measured)	k	Summer	R	Slope	1.46E-04	8.92E-05	-2.85E-05	3.20E-04	704	15,000
Moisture (measured)	k	Summer	R	Intercept	0.012	0.001	0.011	0.013	398	15 000
Moisture (measured)	k	Summer	R	Slope	-3.97E-05	2.54E-05	-9.01E-05	9.95E-06	398	15 000
Air temp. (CHELSA)	k	Summer	R	Intercept	0.011	0.001	0.01	0.012	1403	15 000
Air temp. (CHELSA)	k	Summer	R	Slope	1.72E-04	1.20E-04	-6.58E-05	4.08E-04	1403	15 000
Precip. (CHELSA)	k	Summer	R	Intercept	0.011	0.001	0.01	0.012	1403	15 000
Precip. (CHELSA)	k	Summer	R	Slope	1.07E-05	3.22E-05	-5.23E-05	7.35E-05	1403	15 000
Moisture (ESA)	k	Summer	R	Intercept	0.011	0.001	0.01	0.012	1108	15 000
Moisture (ESA)	k	Summer	R	Slope	-7.21E-07	1.23E-06	-2.90E-04	3.02E-04	1108	15 000
Air temp. (measured)	S	Summer	G	Intercept	0.372	0.009	0.366	0.39	944	15 000
Air temp. (measured)	**S**	**Summer**	**G**	**Slope**	**-0.007**	**0.003**	**-0.014**	**-9.41E-04**	**944**	**15 000**
Soil temp. (measured)	S	Summer	G	Intercept	0.327	0.009	0.309	0.346	715	15 000
Soil temp. (measured)	**S**	**Summer**	**G**	**Slope**	**-0.026**	**0.002**	**-0.031**	**-0.021**	**715**	**15 000**
Moisture (measured)	S	Summer	G	Intercept	0.373	0.015	0.344	0.403	408	15 000
Moisture (measured)	**S**	Summer	G	Slope	-0.001	4.67E-06	-0.002	8.67E-06	408	15 000
Air temp. (CHELSA)	S	Summer	G	Intercept	0.364	0.013	0.338	0.39	1436	8376
Air temp. (CHELSA)	**S**	**Summer**	**G**	**Slope**	**-0.021**	**0.003**	**-0.026**	**-0.016**	**1436**	**8560**
Precip. (CHELSA)	S	Summer	G	Intercept	0.355	0.015	0.326	0.384	1436	15 000
Precip. (CHELSA)	**S**	**Summer**	**G**	**Slope**	**-0.005**	**0.001**	**-0.007**	**-0.004**	**1436**	**15 000**
Moisture (ESA)	S	Summer	G	Intercept	0.297	0.019	0.258	0.334	1128	15 000
Moisture (ESA)	**S**	**Summer**	**G**	**Slope**	**-0.019**	**0.005**	**-0.029**	**-0.008**	**1128**	**15 000**

799

800 **Table S3.** Model outputs for individual environmental variable – summer mass loss polynomial
801 relationships. Bold rows designate polynomial relationships (polynomial parameter) for which
802 the credible interval does not cross zero (i.e., the relationship is "significant"). Sample size
803 indicates number of tea samples available to test relationships. Effective sample size indicates
804 number of convergent models runs. G and R indicate green and rooibos tea, respectively.

Environ. Variable	Decomp. variable	Time period	Tea Type	Parameter	Mean	SD	2.50%	97.50%	Sample size	Effective sample size
Air temp. (measured)	Mass loss	Summer	G	Intercept	0.535	0.00624	0.523	0.547	1913	31625
Air temp. (measured)	Mass loss	Summer	R	Intercept	0.172	0.00634	0.159	0.184	1913	30383
Air temp. (measured)	Mass loss	Summer	G	Slope	0.0078	0.0021	0.00374	0.0119	1913	25671
Air temp. (measured)	Mass loss	Summer	R	Slope	0.00516	0.0021	0.0011	0.00929	1913	27935
Air temp. (measured)	**Mass loss**	**Summer**	**G**	**Polynomial**	**-5.48E-05**	**2.31E-05**	**-0.000101**	**-9.29E-06**	**1913**	**15544**
Air temp. (measured)	Mass loss	Summer	R	Polynomial	-2.48E-05	3.37E-05	-8.99E-05	4.17E-05	1913	15676
Soil temp. (measured)	Mass loss	Summer	G	Intercept	0.617	0.00856	0.6	0.633	1560	17804
Soil temp. (measured)	Mass loss	Summer	R	Intercept	0.215	0.00824	0.199	0.232	1560	18677
Soil temp. (measured)	Mass loss	Summer	G	Slope	0.0201	0.00157	0.017	0.0231	1560	22592
Soil temp. (measured)	Mass loss	Summer	R	Slope	0.0109	0.00153	0.00797	0.0139	1560	21301
Soil temp. (measured)	Mass loss	Summer	G	Polynomial	-0.000642	0.000329	-0.00129	6.70E-06	1560	15355
Soil temp. (measured)	Mass loss	Summer	R	Polynomial	0.000259	0.00032	-0.000375	0.000897	1560	15769
Moisture (measured)	Mass loss	Summer	G	Intercept	0.495	0.0116	0.473	0.518	917	24515
Moisture (measured)	Mass loss	Summer	R	Intercept	0.178	0.0113	0.155	0.2	917	26840
Moisture (measured)	Mass loss	Summer	G	Slope	-0.000848	0.000587	-0.00202	0.000274	917	15676
Moisture (measured)	Mass loss	Summer	R	Slope	-0.000198	0.000499	-0.00117	0.000775	917	16094
Moisture (measured)	**Mass loss**	**Summer**	**G**	**Polynomial**	**5.16E-05**	**1.43E-05**	**2.38E-05**	**8.02E-05**	**917**	**16802**
Moisture (measured)	Mass loss	Summer	R	Polynomial	9.66E-06	1.27E-05	-1.51E-05	3.52E-05	917	17865
Air temp. (CHELSA)	Mass loss	Summer	G	Intercept	0.555	0.0127	0.53	0.58	2837	6177
Air temp. (CHELSA)	Mass loss	Summer	R	Intercept	0.197	0.0119	0.174	0.22	2837	5970
Air temp. (CHELSA)	Mass loss	Summer	G	Slope	0.0166	0.00245	0.0119	0.0214	2837	5759
Air temp. (CHELSA)	Mass loss	Summer	R	Slope	0.0107	0.00216	0.00651	0.015	2837	7225
Air temp. (CHELSA)	Mass loss	Summer	G	Polynomial	0.000197	0.000363	-5.00E-04	0.000934	2837	5128
Air temp. (CHELSA)	Mass loss	Summer	R	Polynomial	0.00031	0.000343	-0.000363	0.000979	2837	6156
Precip. (CHELSA)	Mass loss	Summer	G	Intercept	0.56	0.0165	0.527	0.592	2837	11978
Precip. (CHELSA)	Mass loss	Summer	R	Intercept	0.189	0.0164	0.157	0.221	2837	13451
Precip. (CHELSA)	Mass loss	Summer	G	Slope	0.00384	0.00103	0.00179	0.00585	2837	10612
Precip. (CHELSA)	Mass loss	Summer	R	Slope	0.00174	0.000988	-0.000212	0.00365	2837	12732
Precip. (CHELSA)	Mass loss	Summer	G	Polynomial	1.38E-05	3.94E-05	-6.38E-05	9.10E-05	2837	10820

31

Precip. (CHELSA)	Mass loss	Summer	R	Polynomial	6.33E-05	3.91E-05	-1.26E-05	0.00014	2837	12939
Moisture (ESA)	Mass loss	Summer	G	Intercept	0.601	0.016	0.569	0.632	2234	35778
Moisture (ESA)	Mass loss	Summer	R	Intercept	0.23	0.0162	0.198	0.261	2234	35783
Moisture (ESA)	Mass loss	Summer	G	Slope	0.012	0.00402	0.00413	0.0199	2234	36885
Moisture (ESA)	Mass loss	Summer	R	Slope	0.00781	0.00406	-0.000131	0.0158	2234	37415
Moisture (ESA)	Mass loss	Summer	G	Polynomial	-0.000486	0.00073	-0.0019	0.000944	2234	32330
Moisture (ESA)	Mass loss	Summer	R	Polynomial	0.000236	0.000743	-0.00121	0.00171	2234	30986

805

806 **Table S4.** Model outputs for environmental variable – decomposition relationships within grid
807 cells. Bold rows designate relationships (slope parameter) for which the credible interval does
808 not cross zero (i.e., the relationship is "significant"). Sample size indicates number of tea
809 samples available to test relationships. Effective sample size indicates number of convergent
810 model runs. Variables are standardised within grid cells using mean zero and unit-variance
811 scaling. All models are for summer incubations only. G and R indicate green and rooibos tea,
812 respectively.

| Environmental variable	Decomp variable	Tea Type	Parameter	Mean	SD	2.5%	97.5%	Sample size	Effective sample size
Air temp.	Mass loss	G	Intercept	0.815	0.112	0.595	1.033	1504	4865
Air temp.	Mass loss	R	Intercept	-0.996	0.111	-1.215	-0.782	1504	5131
Air temp.	Mass loss	G	Slope	-0.029	0.036	-0.100	0.041	1504	1964
Air temp.	Mass loss	R	Slope	0.033	0.026	-0.034	0.066	1504	4794
Soil temp.	Mass loss	G	Intercept	0.856	0.122	0.616	1.088	1311	230
Soil temp.	Mass loss	R	Intercept	-0.822	0.120	-1.061	-0.588	1311	137
Soil temp.	**Mass loss**	**G**	**Slope**	**0.144**	**0.027**	**0.091**	**0.197**	**1446**	**261**
Soil temp.	**Mass loss**	**R**	**Slope**	**0.073**	**0.026**	**0.021**	**0.122**	**1446**	**420**
Moisture	Mass loss	G	Intercept	0.816	0.164	0.492	1.132	802	597
Moisture	Mass loss	R	Intercept	-0.877	0.161	-1.191	-0.565	802	817
Moisture	Mass loss	G	Slope	0.049	0.052	-0.054	0.153	802	368
Moisture	Mass loss	R	Slope	0.059	0.046	-0.034	0.151	802	657

813

814 **Table S5.** Model outputs for temperature – decomposition relationships, including an
815 interaction with soil moisture. Bold rows designate relationships (slope parameter) for which
816 the credible interval does not cross zero (i.e., the relationship is "significant"). Sample size
817 indicates number of tea samples available to test relationships. Effective sample size indicates
818 number of convergent model runs. Environmental variables are unscaled and in original units.
819 All models are for summer incubations only. G and R indicate green and rooibos tea,
820 respectively.

Environmental. variable	Decomp. variable	Tea Type	Parameter	Mean	SD	2.5%	97.5%	Sample size	Effective sample size
Measured soil temp. × moisture	Mass loss	G	Intercept	0.522	0.018	0.487	0.558	624	5009
Measured soil temp. × moisture	**Mass loss**	**G**	**Temp. slope**	**0.029**	**0.008**	**0.014**	**0.044**	**624**	**4470**
Measured soil temp. × moisture	**Mass loss**	**G**	**Moisture slope**	**0.002**	**0.001**	**0.001**	**0.004**	**624**	**6430**
Measured soil temp. × moisture	Mass loss	G	Interaction	-1.38e-04	3.32e-04	-5.35e-04	7.86e-04	624	6277
Measured soil temp. × moisture	Mass loss	R	Intercept	0.176	0.016	0.144	0.209	624	6799
Measured soil temp. × moisture	Mass loss	R	Temp. slope	0.008	0.007	-0.004	0.022	624	6349
Measured soil temp. × moisture	Mass loss	R	Moisture slope	0.001	0.001	-0.001	0.002	624	8261
Measured soil temp. × moisture	Mass loss	R	Interaction	4.97e-05	2.81e-04	-5.07e-04	6.05e-04	624	7942
Gridded temp. × moisture	Mass loss	G	Intercept	0.581	0.009	0.563	0.599	2,234	15 000
Gridded temp. × moisture	**Mass loss**	**G**	**Temp. slope**	**0.019**	**0.002**	**0.015**	**0.023**	**2,234**	**15 000**
Gridded temp. × moisture	**Mass loss**	**G**	**Moisture slope**	**0.009**	**0.003**	**0.004**	**0.014**	**2,234**	**15 000**
Gridded temp. × moisture	Mass loss	G	Interaction	0.001	0.001	-6.39e-04	0.002	2,234	15 000
Gridded temp. × moisture	Mass loss	R	Intercept	0.218	0.009	0.201	0.234	2,234	15 000
Gridded temp. × moisture	**Mass loss**	**R**	**Temp. slope**	**0.012**	**0.002**	**0.008**	**0.015**	**2,234**	**15 000**
Gridded temp. × moisture	Mass loss	R	Moisture slope	0.004	0.002	-0.001	0.009	2,234	15 000
Gridded temp. × moisture	**Mass loss**	**R**	**Interaction**	**0.001**	**0.001**	**2.67e-05**	**0.003**	**2,234**	**15 000**

821

822 **Table S6.** Model outputs for relationships between measured environmental variables and
823 gridded environmental variables. Bold rows designate relationships (slope parameter) for
824 which the credible interval does not cross zero (i.e., the relationship is "significant"). Sample
825 size indicates number of sites available to test relationships. Effective sample size indicates
826 number of convergent model runs.

Measured variable	Gridded variable	Parameter	Mean	2.5%	97.5%	Sample size	Effective sample size
Air temperature	CHELSA air temperature	Intercept	-0.225	-1.596	1.194	151	15 000
Air temperature	**CHELSA air temperature**	**Slope**	**0.877**	**0.474**	**1.013**	**151**	**15 000**
Soil temperature	CHELSA air temperature	Intercept	-2.259	-3.507	-1.013	134	15 000
Soil temperature	**CHELSA air temperature**	**Slope**	**1.24**	**1.130**	**1.352**	**134**	**15 000**
Soil moisture	CHELSA precipitation	Intercept	16.876	14.625	19.197	79	15 000
Soil moisture	**CHELSA precipitation**	**Slope**	**-0.120**	**-0.170**	**-0.074**	**79**	**11 445**
Soil moisture	ESA soil moisture	Intercept	24.405	22.237	26.612	39	15 000
Soil moisture	ESA soil moisture	Slope	0.061	-0.004	0.128	39	15 000

827

Supplementary Figures
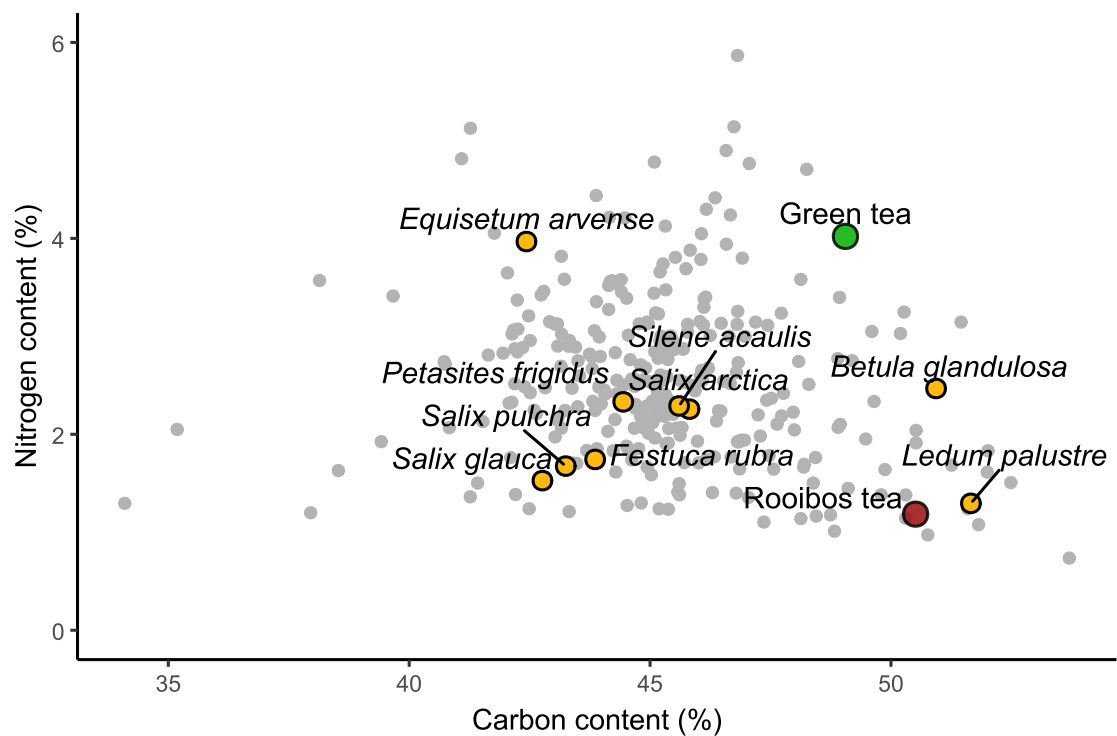
Figure S1. Carbon and nitrogen content of green and rooibos tea compared a range of representative tundra species. Tea types are indicated by red (rooibos tea) and green (green tea) plots. Yellow dots and corresponding names indicate tundra species for which we collected and run the incubation experiment presented in Fig. 2. Grey dots represent a tundra species with available data from the Tundra Trait Team Database [94,95].
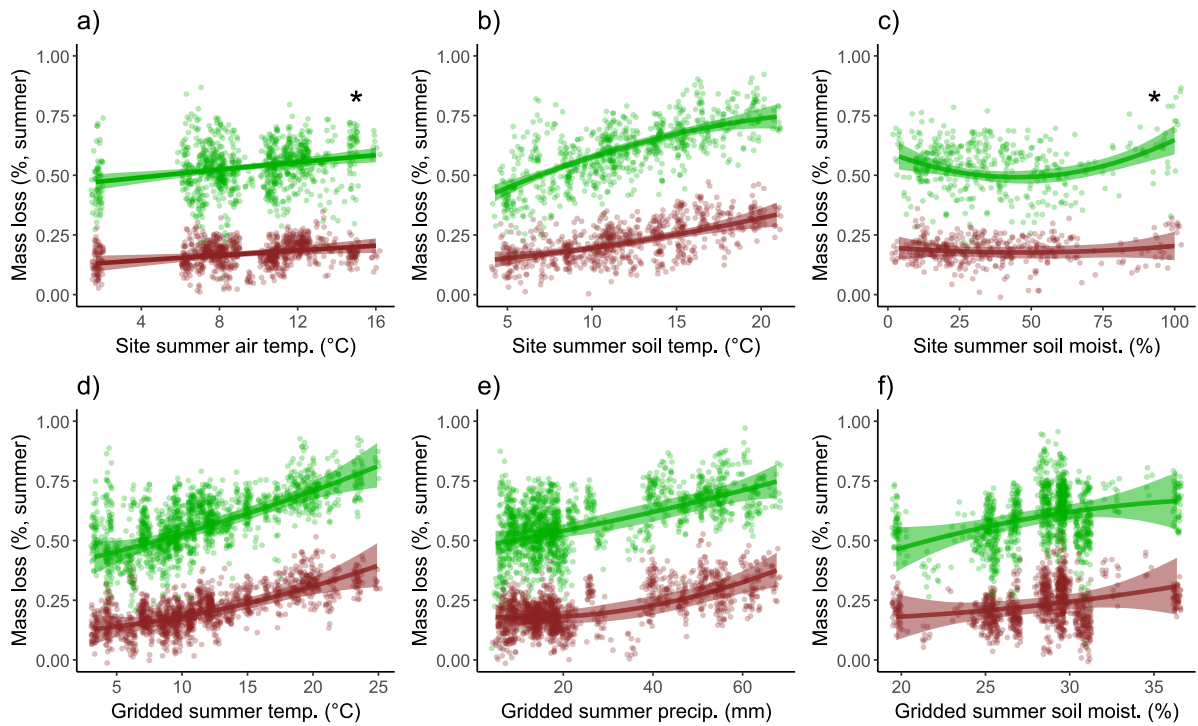
Figure S2. Polynomial relationships between decomposition (mass loss), measured environmental variables (a-c) and gridded climate data (d-f) for summer tea incubations. Points indicate individual tea bag replicates across all sites. Lines indicate hierarchical Bayesian polynomial model fits with 95% credible intervals. Colours indicate tea type (red = rooibos tea, green = green tea). See Table S3 for model outputs. Polynomial parameters with 95% credible interval not including 0 are highlighted with (*).
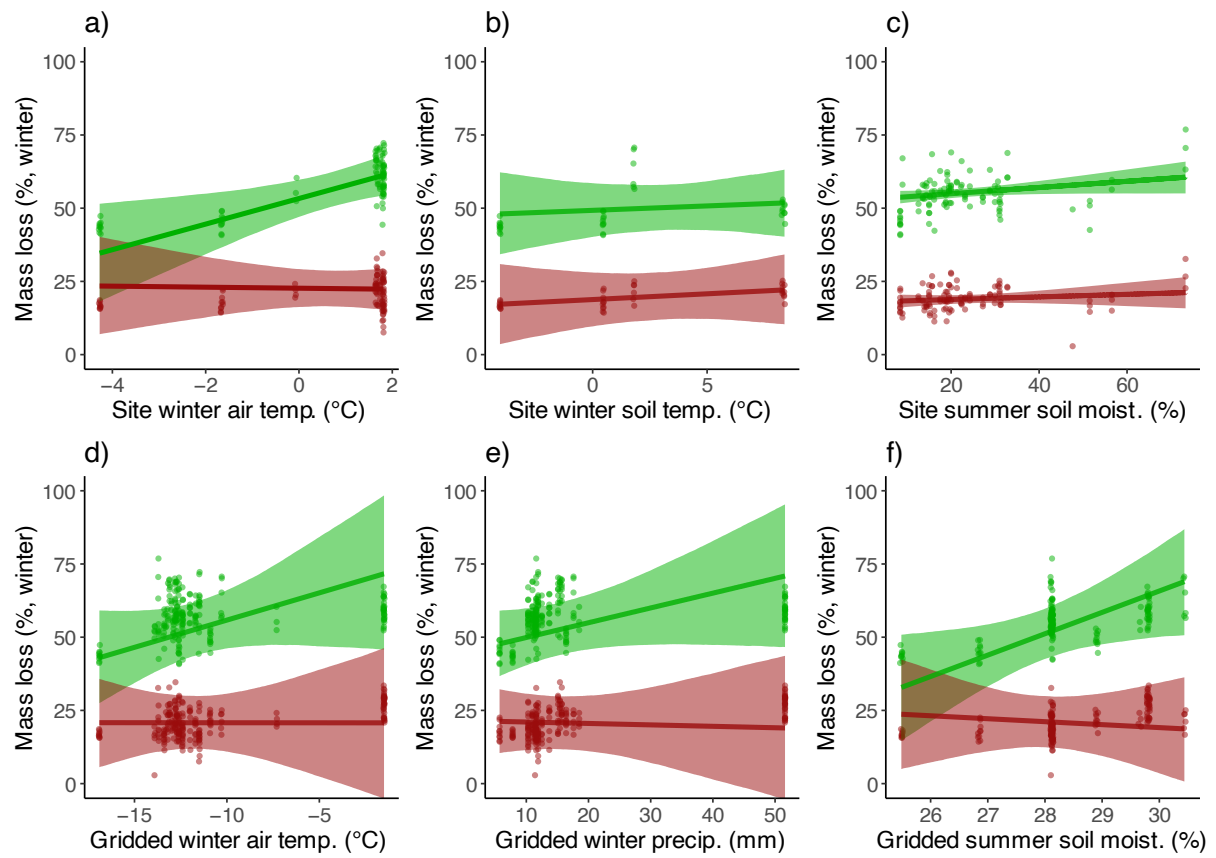
Figure S3. Relationships between decomposition (mass loss), measured environmental variables (a-c) and gridded climate data (d-f) for winter tea incubations, as opposed to summer incubations in main text (Fig. 3) or year-long incubations (Fig. S4). Points indicate individual tea bag replicates across all sites. Lines indicate hierarchical Bayesian model fits with 95% credible intervals. Colours indicate tea type (red = rooibos tea, green = green tea). See Table S2 for model outputs.
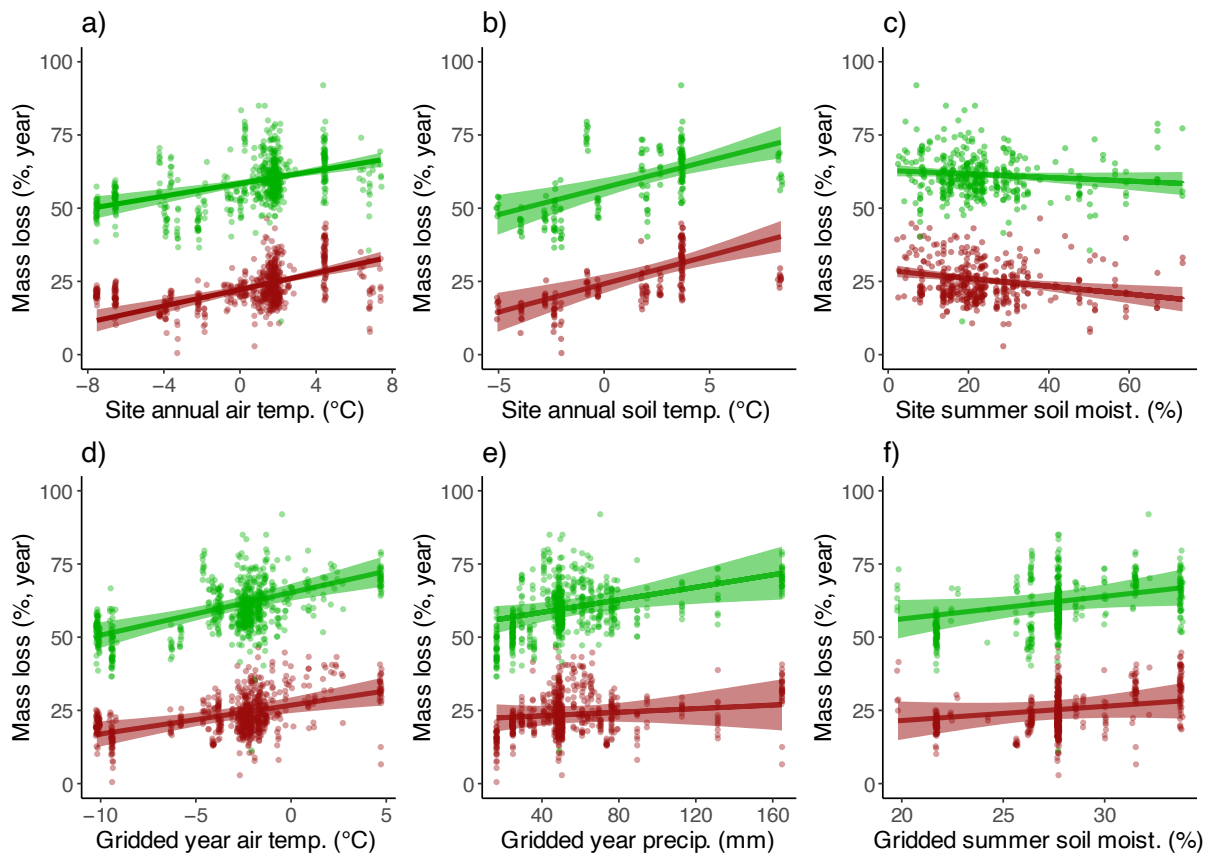
Figure S4. Relationships between decomposition (mass loss), measured environmental variables (a-c) and gridded climate data (d-f) for year-long tea incubations, as opposed to summer incubations in main text (Fig. 3) or winter incubations (Fig. S3). Points indicate individual tea bag replicates across all sites. Lines indicate hierarchical Bayesian model fits with 95% credible intervals. Colours indicate tea type (red = rooibos tea, green = green tea). See Table S2 for model outputs.
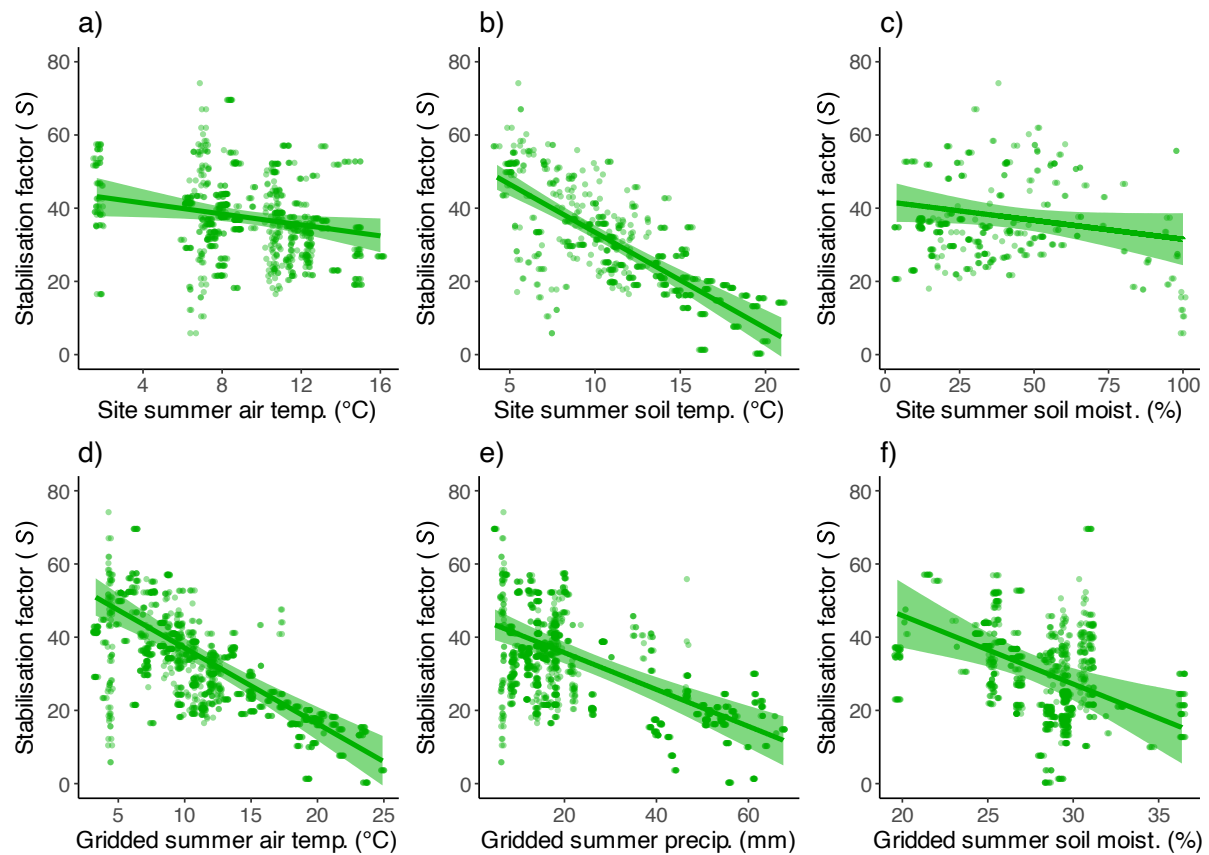
Figure S5. Relationships between stabilisation factor (S), measured environmental variables (a-c) and gridded climate data (d-f) for summer tea incubations, as opposed to summer mass loss in main text (Fig. 3). S is calculated based on decomposition of green tea, and is assumed to be consistent across tea types[19]. S represents the proportion of labile material remaining once decomposition has stabilised, and thus long-term carbon storage. Points indicate individual tea bag replicates across all sites. Lines indicate hierarchical Bayesian model fits with 95% credible intervals. See Table S2 for model outputs.
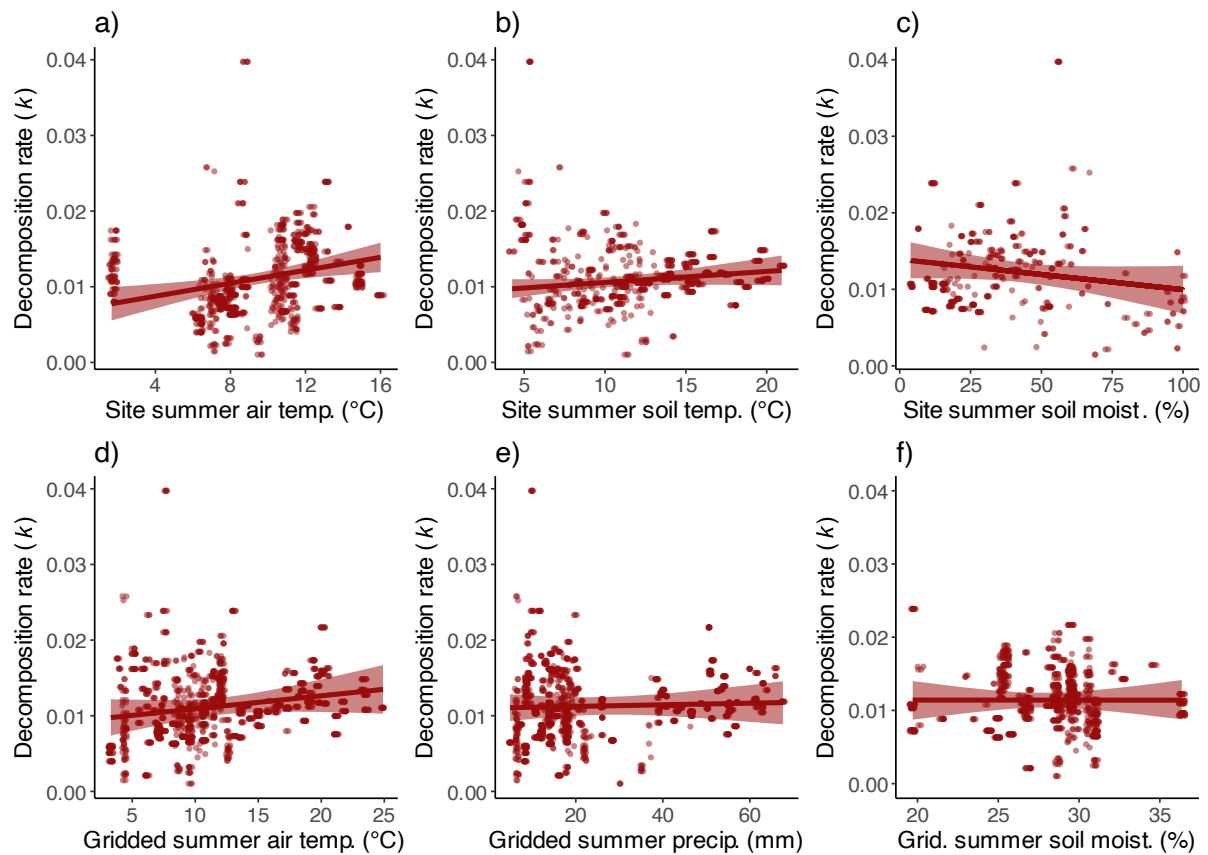
Figure S6. Relationships between decomposition rate (k), measured environmental variables (a-c) and gridded climate data (d-f) for summer tea incubations, as opposed to summer mass loss in main text (Fig. 3). k is calculated based on decomposition of rooibos tea, and is assumed to be consistent across tea types[19]. k represents the rate of loss of labile material, and thus short-term decomposition dynamics and biogeochemical cycling. Points indicate individual tea bag replicates across all sites. Lines indicate hierarchical Bayesian model fits with 95% credible intervals. See Table S2 for model outputs.

880

881
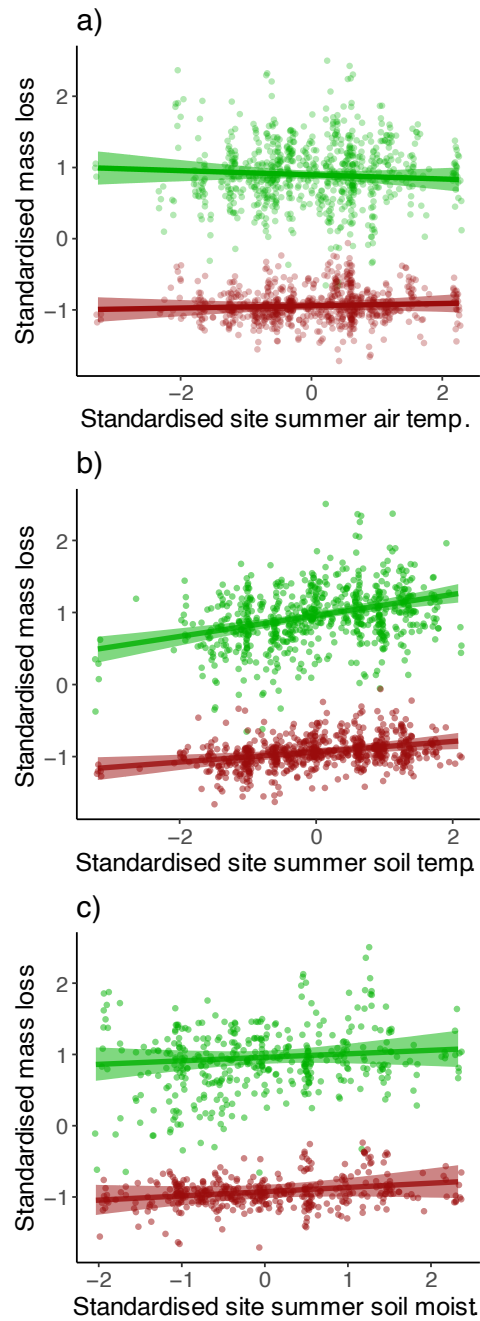
Figure S7. Within-grid cell relationships reflect among-site relationships between environmental variables and mass loss, but with greater variability. Within-grid cell relationships between summer decomposition (mass loss) and measured environmental variables, as opposed to among sites in main text (Fig. 3). Environmental and decomposition variables are standardised within 0.25 × 0.25-degree resolution grid cells using mean zero and unit-variance scaling. Points indicate individual tea bag replicates. Lines indicate hierarchical Bayesian model fits with 95% credible intervals. Colours indicate tea type (red = rooibos tea, green = green tea). See Table S3 for model outputs.

890

891
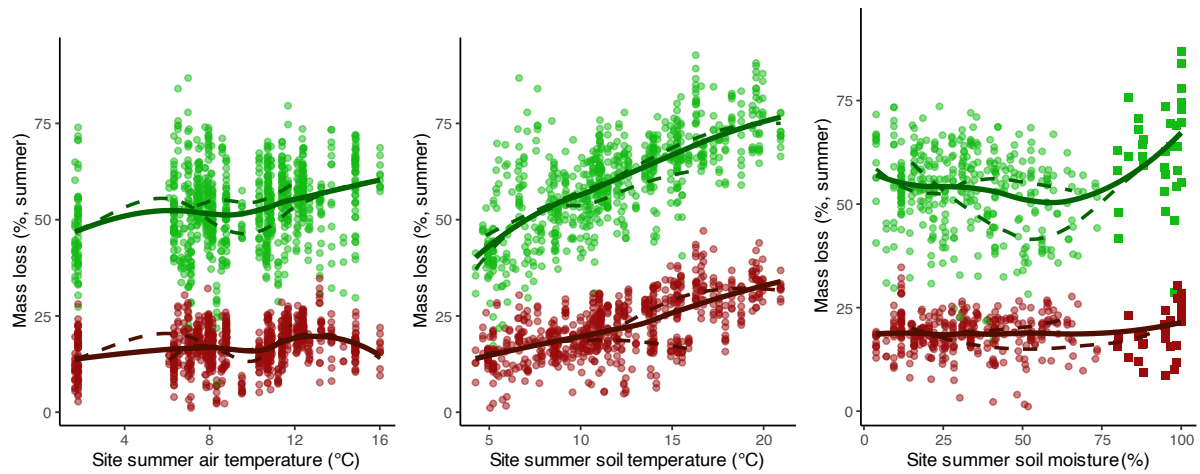
Figure S8. Overall, relationships between climate variables and mass loss were best described by linear rather than exponential models. In order to test the linearity of the relationships between climate variables and mass loss of tea types, we fit general additive models with a loess fit to the overall dataset (solid lines) and to the Western and Eastern hemispheres as two subsets of the data (dashed lines). The relationship between site summer soil moisture and green tea mass loss was more exponential, but this was driven by data from Svalbard located at particularly wet sites (square points) and thus we do not have confidence that the exponential relationships can be generalised to the tundra biome, which were better fit by hierarchical linear models (Fig. 3).
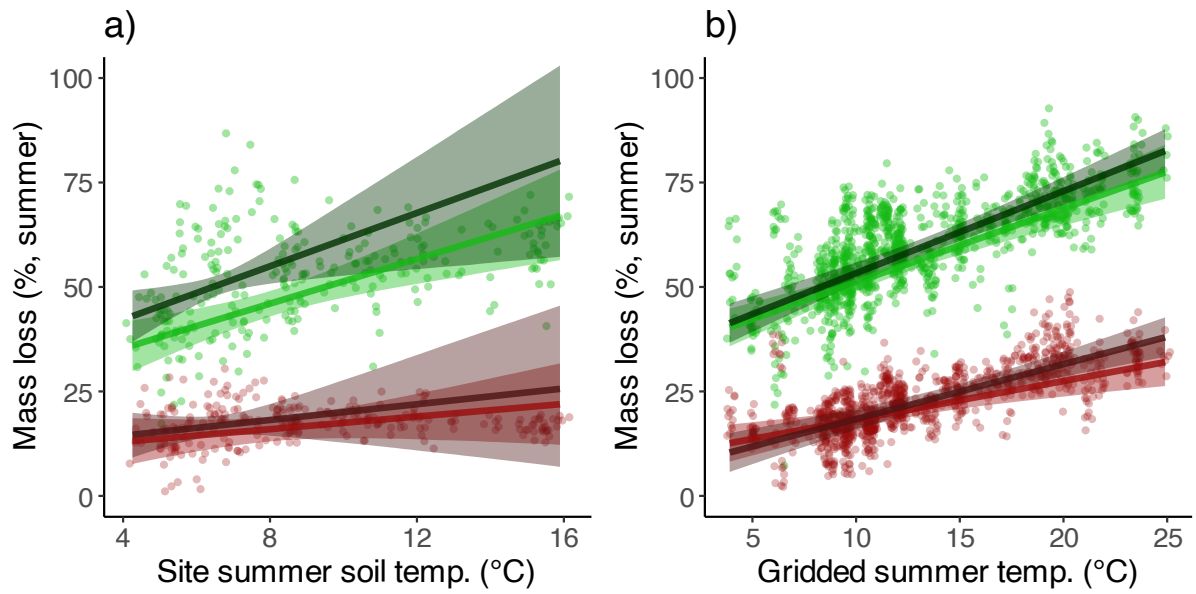
**Figure S9.** Soil moisture did not influence the relationships between soil temperature and mass loss, but decomposition was higher at wetter versus drier sites at any given temperature. Relationships between summer decomposition (mass loss), (a) measured soil temperature and soil moisture, and (b) gridded temperature (CHELSA) and soil moisture (ESA). Models incorporate the interaction between soil temperature and soil moisture. Lines indicate predicted decomposition at upper (dark) and lower (light) quartiles of soil moisture, representing wet and dry sites respectively, based on hierarchical Bayesian model fits with 95% credible intervals. Points indicate individual tea bag replicates. Colours indicate tea type (red = rooibos tea, green = green tea). See Table S4 for model outputs.
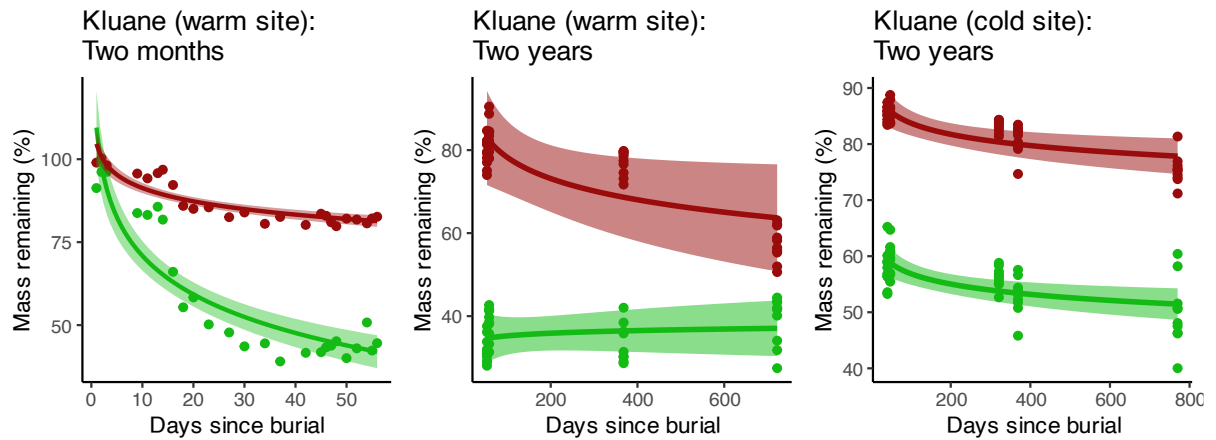
912

913

914 **Figure S10.** Mass loss of tea types did not converge after two years and stabilised after
915 approximately 30 days. Mass remaining over time of rooibos and green tea at warm and cold
916 tundra sites at the Kluane Lake location (see Table S1). Mass loss is calculated using a single-
917 phase exponential decay decomposition model. (a) Mass remaining at the warm experimental
918 site, with tea extracted every two days over a two-month summer period; (b) mass remaining
919 at the warm experimental site with summer, one-year and two-year incubation lengths; and
920 (c) mass remaining at the cold experimental site with summer, two-month, one-year and two-
921 year incubation lengths.
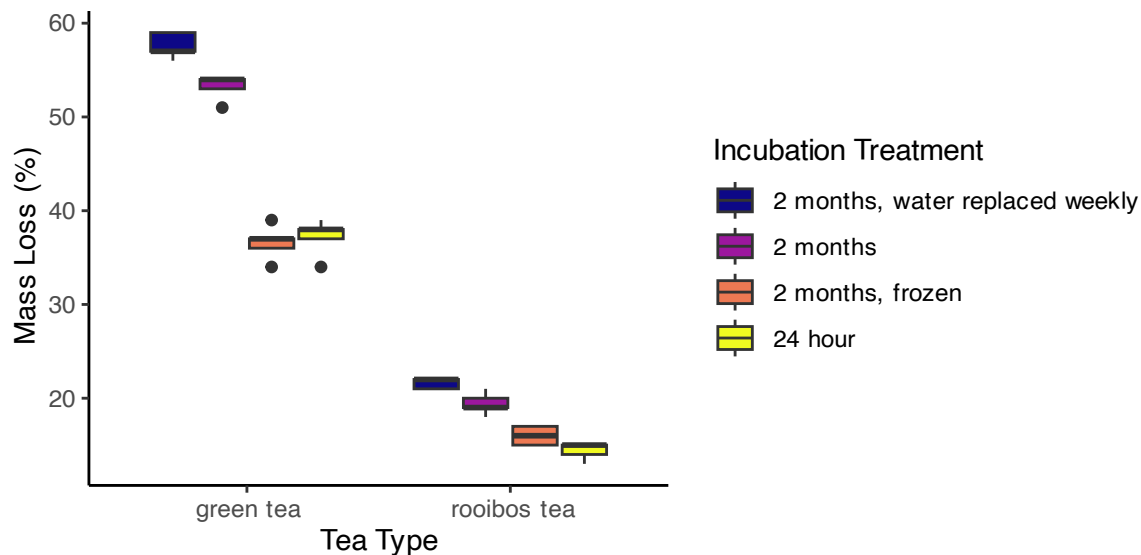
922

923

924 **Figure S11.** In order to test the influence of leaching, we conducted 2-month and 24-hour
925 incubations of green and rooibos tea in a laboratory environment at room temperature, in a
926 4°C fridge and a 20°C freezer. We found ~20% greater mass loss for green tea and ~7%
927 greater mass loss for rooibos tea in two-month incubations rather than in 24-hour incubations
928 in liquid water. Leaching was not strongly influenced by replacement of water and was slower
929 in frozen conditions for green and rooibos tea.
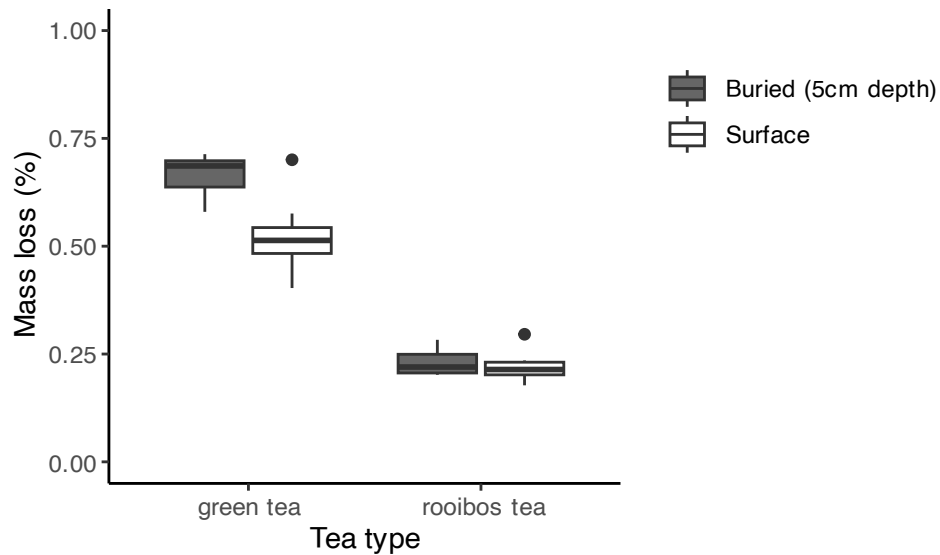
Figure S12. Mass loss of buried tea bags was significantly greater than tea placed on the ground surface for green tea, but not different for rooibos tea. Teabags were incubated in a common site (Kluane Lake, see Table S1) and were either buried at 5 cm depth directly in the soil (grey) or placed within a litter bed and covered in a local litter medium (white), following protocols outlined in Cornelissen et al. (2007). Teabags were incubated for one year, though the time periods of incubation differed between the two treatment types (buried: June – June, surface: August – August) as tea bags are taken from two different, but adjacent, experiments. Stars indicate significance (***, P < 0.001, ns, P > 0.05, t-test).

940

941
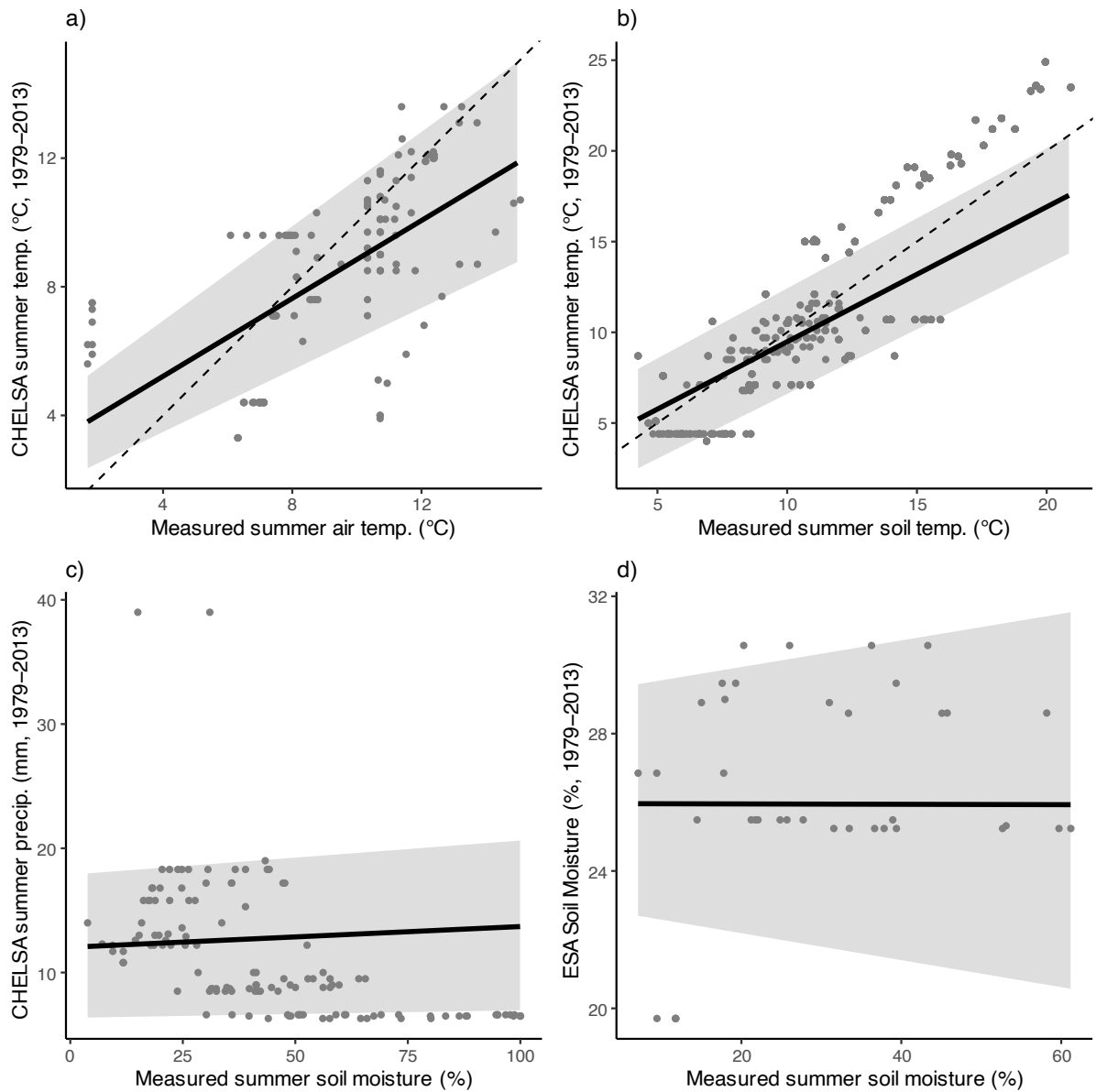
Figure S13. Site-measured environmental variables aligned with gridded climate variables for summer temperature, but not summer soil moisture. Relationships between site-measured environmental variables and gridded climate data for all tea bag sites with available data. Lines indicate hierarchical Bayesian model fits and errors are 95% credible intervals. See Table S5 for model outputs.

947
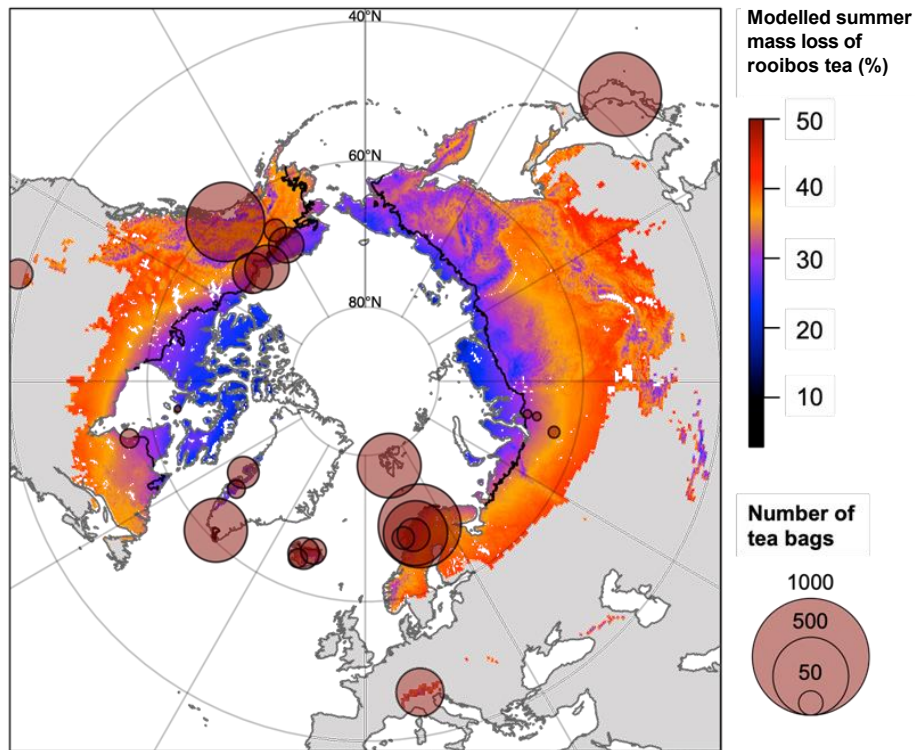
Figure S14. Modelled summer decomposition (percent mass loss) of rooibos tea for tundra and sub-Arctic regions based on 1979 to 2013 mean summer air temperature (Climatologies at high resolution for the Earth's land surface, CHELSA) and soil moisture (European Space Agency data, ESA) from 1979 to 2013. Field collection locations are illustrated by red circles, grouped by geographic region (Table S1, figure excludes Australian alpine region). Circle size indicates the number of tea bag replicates within each geographic region. Tundra and sub-Arctic classifications are based on Köppen-Geiger classification[47]. Ice-covered areas are excluded. The circum-Arctic treeline is indicated with a black line[48].